



# Review of the fuel properties, characterisation techniques, and pre-treatment technologies for oil palm empty fruit bunches

Bemgba B. Nyakuma<sup>1</sup> · Syie L. Wong<sup>1</sup> · Olagoke Oladokun<sup>1,2</sup> · Aliyu A. Bello<sup>2</sup> · Hambali U. Hambali<sup>1</sup> · Tuan Amran T. Abdullah<sup>1</sup> · Keng Y. Wong<sup>3</sup>

Received: 16 July 2020 / Revised: 23 October 2020 / Accepted: 6 November 2020 / Published online: 23 November 2020  
© Springer-Verlag GmbH Germany, part of Springer Nature 2020

## Abstract

The valorisation of oil palm empty fruit bunches (OPEFB) in the palm oil industry is hampered by major challenges due to its poor fuel properties, which require comprehensive characterisation and pre-treatment. This paper presents an overview of the various technologies currently employed for the fuel characterisation and pre-treatment of OPEFB in the literature. Furthermore, the paper presents the current challenges and prospects of OPEFB characterisation and pre-treatment techniques. The reviews indicate that OPEFB characterisation studies in the literature are limited to the chemical, thermal, kinetic, and thermodynamic fuel properties. The authors opine that future characterisation studies are required to examine the physical, morphological, and microstructural properties of OPEFB. The paper also notes that drying, size reduction, and pelletisation are the most common pre-treatment techniques for OPEFB. The various characterisation and pre-treatment techniques highlighted are prone to various limitations, which indicate that more effective strategies are required to save the energy, time, and cost for future OPEFB valorisation. The design, implementation, or adoption of hybrid biomass pre-treatment and conversion systems could effectively address the issues of poor OPEFB fuel properties, operational challenges, and product distribution.

**Keywords** Fuel characterisation · Pre-treatment techniques · Oil palm · Empty fruit bunches

## 1 Introduction

The oil palm tree (*Elaeis guineensis* Jacq.) is a tree crop native to West and Central Africa [1]. It is now cultivated commercially in Indonesia, Malaysia, Thailand, and Colombia owing to its heliophytic nature [2]. Historically, oil palm was first introduced into Malaysia as an ornamental plant in the nineteenth century [3]. Over the years, oil palm has been transformed into a major agricultural commodity in Malaysia [4, 5], where it is cultivated for the production of crude palm oil (CPO) and other palm oil-related products [6]. The production

of CPO has experienced geometric growth from 2.5 million tonnes in 1980 to 20 million tonnes to date, thereby reinforcing Malaysia's position as a prominent stakeholder in the global edible oil market [7]. Malaysia accounts for about 30% of the global production and trade in CPO, which generates significant socio-economic and technological benefits for the country [5]. According to the Agency for Innovation in Malaysia (AIM), CPO production accounts for about 8% of Malaysia's gross national income (GNI) [8]. The palm oil industry also accounts for a significant proportion of the direct or indirect employment of numerous individuals and communities in the country [9]. It is also a major source of raw materials for the manufacture of biofuels, oleo-chemicals, and pharmaceuticals [10, 11].

The demand for CPO and palm kernel oil (PKO) has soared over the years along with the concomitant increase in the cultivation of oil palm in Malaysia, which currently spans over 5.9 million hectares of land [12]. According to the Malaysian Palm Oil Board (MPOB) [12], the palm oil industry produced 19.5 million tonnes of CPO along with 2.29 million tonnes of PKO in 2019. Furthermore, the export trade in palm oil and its derived products comprising CPO (66.26%), oleo chemicals

✉ Bemgba B. Nyakuma  
bbnyax1@gmail.com

<sup>1</sup> School of Chemical and Energy Engineering, Faculty of Engineering, Universiti Teknologi Malaysia, 81310 Skudai, Johor, Malaysia

<sup>2</sup> Department of Chemical Engineering, University of Maiduguri, P.M.B 1069 Bama Road, Maiduguri, Borno State, Nigeria

<sup>3</sup> School of Mechanical Engineering, Faculty of Engineering, Universiti Teknologi Malaysia, 81310 Skudai, Johor, Malaysia

(12.43%), Palm kernel cake (9.22%), and PKO (3.71%) along with biodiesel and other finished products amounted to 24.87 million tonnes cumulatively valued at RM41 billion [12]. Despite its socio-economic and technological importance, CPO production along with the large-scale expansion of oil palm cultivation have created significant environmental problems in Malaysia.

The oil palm industry in Malaysia generates 80–100 million dry tonnes of solid-based oil palm wastes (OPW) annually [13]. Based on the source of origin, the OPWs are broadly categorised into oil mill and plantation-based solid wastes. The plantation-based wastes consist of oil palm fronds (OPF) and oil palm trunks (OPT), which collectively account for over half of all the solid wastes generated from the industry [14]. Conversely, the remainder is derived from the processing of fresh fruit bunches (FFB), which consists of oil palm empty fruit bunches (OPEFB), palm kernel shell (PKS), and palm mesocarp fibres (PMF) in palm oil mills. Typically, the percentage distribution of solid OPW generated from palm oil mills after CPO and KPO extraction are OPEFB (22–23%), PKS (5.5–7%), and PMF (13.5–15%) based on the residue-to-product ratios [14, 15]. It is estimated that about 17 million tonnes of OPEFB, 5.9 million tonnes of PKS, and 9.6 million tonnes of PMF are generated annually on average in Malaysia [16, 17]. Figure 1 presents an overview of the distribution of solid wastes generated by the oil palm industry.

The largest fraction of OPWs generated from the palm oil mills is the oil palm empty fruit bunches (OPEFB). It is estimated that for every 1 kg of CPO produced, 1 kg of OPEFB is generated as solid waste residue. OPEFB is the bulky brown heterogeneous residue generated after the sterilisation and stripping of oil palm fresh fruit bunches during the production of CPO [18]. In its raw unprocessed form, OPEFB is characterised by high moisture, ash, and mineral matter contents along with low calorific value and bulk density [19]. Due to these reasons, OPEFB is considered a low economic value, feedstock material, and boiler fuel utilised primarily as organic manure, composting, or mulching material in oil palm plantations [14, 20, 21]. The low conversion efficiencies of these strategies have resulted in the accumulation of large stockpiles of OPEFB thereby increasing the costs of processing, disposal, and management of the wastes [22]. The poor properties of OPEFB have significantly hampered its sustainable valorisation into clean energy and value-added products.

It is evident that if left unchecked, the current unsustainable waste disposal and management practices in the industry could aggravate environmental pollution and stall progress towards mitigating greenhouse gas emissions, land degradation, and loss of biodiversity in the country. Given the impending challenges, the government of Malaysia established the National Biomass Strategy (NBS). The policy aims to explore socially acceptable, low cost, and

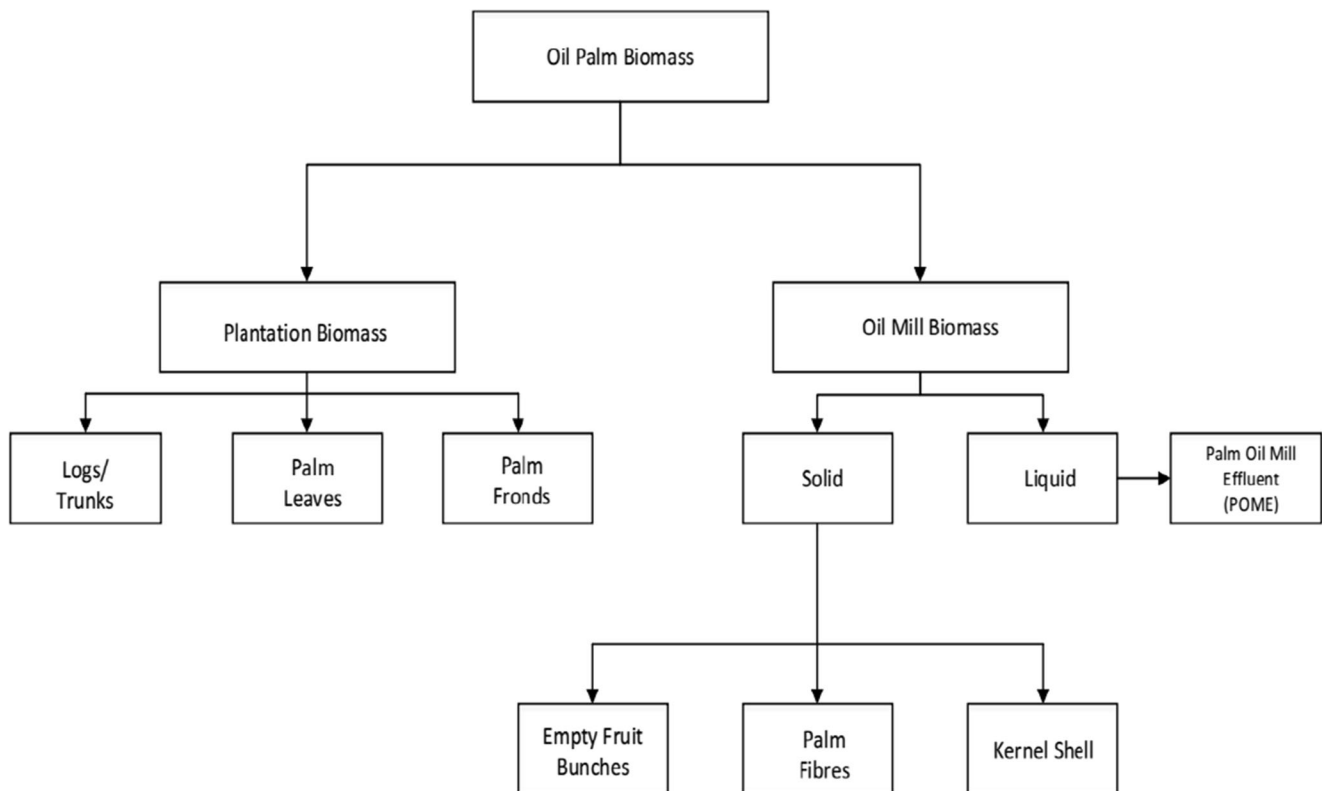


Fig. 1 Sources of oil palm wastes

environmentally friendly technologies for valorising the nation's large stockpiles of solid oil palm wastes generated annually. The long-term objective is to also generate RM 30 billion from OPW into higher-value products, reduce GHG emissions, and create 66,000 jobs. It is envisaged that the initiative will identify, examine, and highlight the biomass and bioenergy potential of OPW for application in future clean, renewable, and sustainable energy applications [13].

Numerous researchers have extensively identified, examined, and reported on various biochemical and thermochemical processes for the valorisation of OPW particularly OPEFB in the literature. The most commonly employed techniques for OPEFB valorisation include torrefaction [23, 24], pyrolysis [25, 26], hydrothermal carbonisation [27, 28], liquefaction [29, 30], gasification [31–33], and combustion [34–36]. Other studies have investigated the valorisation of OPEFB through biochemical approaches [37–39]. According to the findings, thermochemical OPEFB conversion through low-temperature processes (LTP) such as torrefaction, pyrolysis, HTC, and liquefaction results in low mass yields and conversion inefficiencies. Additionally, the liquid products are characterised by highly oxygenated or corrosive tar fractions that require further pre-treatment, conditioning, and processing.

In contrast, the high-temperature processes (HTP) of gasification and combustion of OPEFB generate fuel/flue gas mixtures that could be directly utilised in power generation equipment with minimal processing. Nonetheless, the HTP are prone to sintering, agglomeration, fouling, and tar formation along with low syngas heating value, yield, and distribution during conversion. The outlined problems are largely ascribed to the fuel properties of OPEFB such as high-moisture and alkali–alkali earth metal (AAEM) content and its low bulk density, heterogeneity, and hygroscopicity [40, 41]. Therefore, the pre-treatment, characterisation, and conditioning of OPEFB are required to improve its fuel properties for higher conversion efficiencies and effective yield and distribution of products. These processes could potentially improve the effectiveness of current technologies and future strategies for the disposal and management of OPEFB in the oil palm industry [14, 42].

Previous researchers have presented comprehensive reviews on the bioenergy and biofuel potentials of OPEFB through gasification [43–45] and pyrolysis [19, 46], along with hydrothermal [47, 48], chemical [49, 50], and enzymatic treatments [51, 52]. Other studies have reviewed the prospects of utilising OPEFB as sustainable biomaterials in hydrogel [53], coatings [54], natural fibres [55], and polymeric composites [56, 57]. The title search of studies on OPEFB in the Web of Science (WoS) core collection from 1970 to 2019 revealed a total of 494 records comprising 384 articles, 108 proceedings, 7 reviews, and other materials specific to OPEFB. However, the outlined review papers primarily

highlight the biomaterials, bioenergy, and biofuel applications of OPEFB without comprehensive insights into the physical, chemical, thermal, and kinetic properties of OPEFB determined through characterisation and pre-treatments. Therefore, this paper presents a review of the characterisation techniques and pre-treatment technologies for oil palm empty fruit bunches (OPEFB). The paper also presents an overview of the fuel properties of OPEFB based on the various chemical, thermal, and kinetic characterisation techniques employed by researchers in the literature. The various experimental methods, standards, and equipment for the characterisation and pre-treatment of OPEFB are also presented. It is envisaged that this review will address the gap in knowledge on the characterisation techniques and pre-treatment technologies typically employed to examine the solid fuel properties of OPEFB in the literature.

## 2 Characterisation techniques

The fuel characterisation of potential biomass feedstock is required to assess its quality, quantity, and energy potential using standardised laboratory tests [58, 59]. The characterisation techniques are also used to predict and estimate the product yield, compositional profiles, or potential emissions from biomass conversion [60]. Furthermore, the fuel characterisation of potential biomass feedstock is critical to the design, optimisation, and scale-up of biomass conversion processes. The major tests for characterising the chemical, thermal, kinetic, and thermodynamic fuel properties of potential biomass feedstock for thermochemical conversion will be highlighted next.

### 2.1 Chemical properties

The chemical properties of any potential biomass feedstock consist of all the organic and inorganic structural constituents used to examine its energy content and product yield. Due to the complexity of biomass composition, it is important to characterise its constituents for a better understanding of the effects of conversion. The key characterisation techniques for examining the chemical fuel properties of biomass include ultimate, proximate, calorific (higher heating value, HHV), and metal oxide composition analyses.

#### 2.1.1 Ultimate analysis

This is a measure of the elemental composition of feedstock biomass, as derived from the mathematical relation in weight per cent (wt. %) [61, 62];

$$C + H + N + S + O = 100\% \quad (1)$$

The terms C, H, N, S, and O represent the carbon, hydrogen, nitrogen, sulphur, and oxygen contents, respectively, as determined from an elemental analyser in weight percentage based on ASTM D5291. The ultimate (elemental) analysis of OPEFB has been examined by various researchers in the literature as presented in Table 1 based on its constituent elements; C—carbon; H—hydrogen; N—nitrogen; S—sulphur; and O—oxygen in weight percentage.

As observed, the carbon (C) content of OPEFB can typically range from 40.70 to 49.50 weight percentage or an average of 45.85 wt%. The hydrogen (H) is from 4.03 to 7.33 wt% or an average of 6.20 wt%, whereas oxygen (O) could be from 38.29 to 50.57 wt% or an average of 45.07 wt%. Nitrogen (N) is from 0.00 to 1.96 wt% or an average of 0.79 wt% whereas sulphur (S) can range from 0.00 to 1.10 wt% or an average of 0.36 wt% for OPEFB in the literature. The elemental composition of potential biomass feedstock, particularly, the content of C, H, and O, is crucial to the planning, design, and development of biomass conversion processes. It is also critical to computing the feedstock feed rates and reaction gas requirements (e.g. air factors, equivalence ratios, and steam requirements) in process equipment such as gasifiers and combustors (boilers) [76, 77]. Furthermore, the energy content (higher heating value, HHV), as well as the emission profiles and waste characteristics, is also estimated from biomass elemental composition using empirical relations proposed by researchers in literature [78, 79].

### 2.1.2 Proximate analysis

This is the fuel composition of biomass measured in terms of its moisture content (MC), volatile matter (VM), ash (AC), and fixed carbon (FC), as expressed in weight per cent (wt. %) [61, 80]. The MC is the gross content of inherent (equilibrium) and external (free) water present in biomass, whereas VM comprises the condensable and non-condensable gaseous components released during biomass conversion. The AC represents the inorganic solid residue that typically consists of the alkali–alkali earth metals (AAEM) from biomass combustion. The FC is the solid carbonaceous material or char resulting from devolatilisation during biomass pyrolysis. The compositions of MC, VM, and AC are derived experimentally from various ASTM standards reported in the literature [61, 80]. The MC can be either empirically determined from the ASTM Standards D-3173 or E-871, which require heating a known mass of the biomass in a muffle furnace or oven at 105 °C until constant weight. The mass loss is subsequently computed as the MC of the biomass. The volatile matter is determined from the ASTM Standards D-3175 or E-872, based on the mass loss from heating the biomass sample at 950 °C for 7 min in an oven or muffle furnace. The AC content is computed from heating a known mass of the biomass-based on the procedures of the ASTM Standards D-3174 or D-1102 in a muffle furnace at 700 °C. Alternatively, the proximate properties of biomass feedstock can be deduced from thermogravimetric analysis (TGA) [81].

**Table 1** Ultimate (elemental) properties of OPEFB

C (wt%)	H (wt%)	N (wt%)	S (wt%)	O (wt%)	References
48.79	7.33	0.00	0.68	40.18	Yang et al. [63]
49.07	6.48	0.70	0.10	38.29	Abdullah, Gerhauser [64]
48.79	7.33	0.00	0.68	40.18	Li et al. [65]
43.52	5.72	1.20	0.66	48.90	Lahijani, Zainal [41]
46.62	6.45	1.21	0.04	45.66	Mohammed et al. [66]
40.70	5.40	0.30	1.10	47.00	Madhiyanon et al. [34]
45.00	6.40	0.25	1.06	47.30	Langè, Pellegrini [67]
48.30	6.66	1.00	0.34	43.70	Parshetti et al. [68]
49.50	5.90	0.00	0.50	40.60	Johari et al. [69]
43.62	4.03	1.96	0.17	50.22	Chan et al. [70]
46.62	6.45	1.21	0.04	45.66	Aziz et al. [71]
45.01	4.88	0.78	0.31	49.02	Chuah et al. [72]
48.20	6.10	1.30	0.20	38.30	Nakason et al. [73]
42.08	7.00	0.99	0.00	49.90	Ariffin et al. [31]
46.77	6.84	0.71	0.29	45.39	Hantoko et al. [74]
44.72	6.58	0.80	0.17	42.96	Yan et al. [75]
45.23	6.00	1.21	0.13	47.43	Nyakuma et al. [42]
42.82	6.07	0.54	0.00	50.57	Sukiran et al. [24]

The FC is typically determined by difference using the relation for proximate analysis [61, 82];

$$FC = 100\% - (MC + VM + AC) \tag{2}$$

Table 2 presents the proximate properties of OPEFB based on MC—moisture; VM—volatile matter; AC—ash content; and FC—fixed carbon in the literature.

Based on Table 2, the moisture content (MC) of OPEFB is typically in the range from 0.00 to 60 wt% or 12.45 wt% on average, whereas the VM is between 66.10 and 83.86 wt% or 76.72 wt%. Furthermore, the ash content (AC) ranges from 3.00 to 7.70 wt% or 4.54 wt% on average, whereas the fixed carbon (FC) is typically in the range 8.36 to 28.40 wt% or 14.98 wt% on average. The proximate analysis is also an important technique for examining the energy content of potential biomass feedstock. Several authors have processed empirical relations to compute the higher heating values (HHV) of biomass feedstock based on its proximate properties such as MC, VM, AC, and FC [85–87]. This approach provides a quick, cheap, and reliable technique to compute the energy content of biomass, particularly where standard bomb calorimetric analysis cannot be utilised.

### 2.1.3 Lignocellulosic analysis

The structure of biomass typically consists of three major polymeric components, namely, hemicellulose, cellulose,

and lignin. Other major constituents include ash and extractives (such as oils, proteins, starch). The composition of the lignocellulosic components differs significantly based on the type, age, plant part, and source of the biomass [61]. Figure 2 presents a pictorial depiction of the basic biomass components.

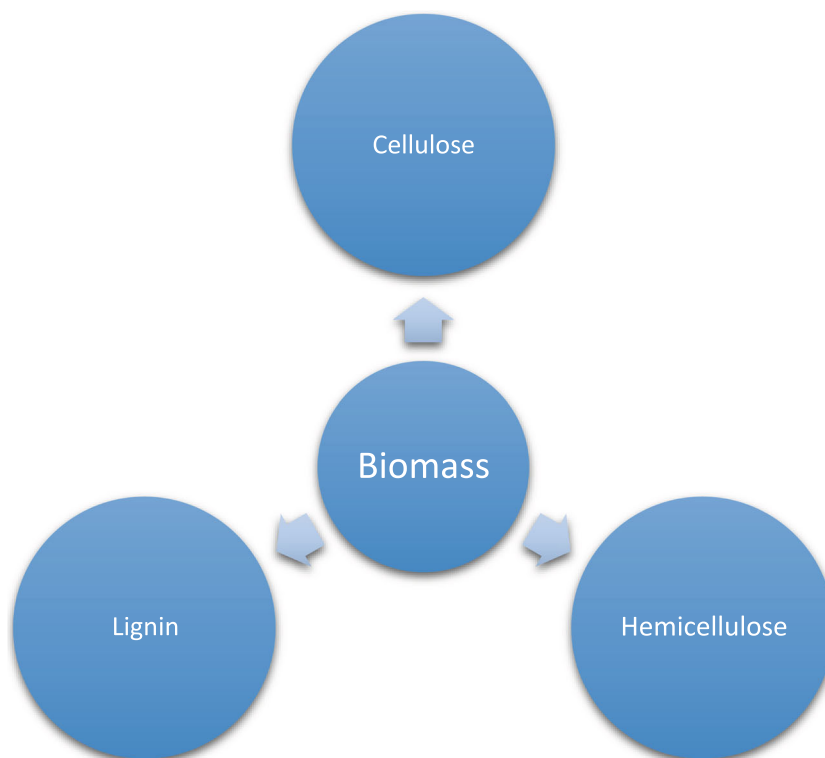
Cellulose is considered the most abundant biopolymer or organic compound on the planet formed by the process of photosynthesis. It is a linear polymer with long chains that consist of β-1,4-linked glucose units arranged in alternate orientation [88]. Chemically, it is denoted by the empirical formula (C<sub>6</sub>H<sub>10</sub>O<sub>5</sub>)<sub>n</sub> along with a high polymerisation and molecular weight of ~ 10,000 and ~ 500,000 g/mol, respectively [61]. Structurally, cellulose accounts for 30–90% by weight of most plants [61], thereby providing crystallinity, strength, and rigidity for the skeletal structure of plants [89]. Due to its chemical and structural properties, cellulose is heterogeneous, highly insoluble, and resistant to enzymatic hydrolysis [90, 91]. Although thermally stable, it can undergo decomposition or devolatilisation between 275 and 350 °C to form the monomer levoglucosan, volatiles, tar, and other condensable vapours [92, 93].

In contrast, hemicellulose is an amorphous polymer with a branched-chain structure and lower level of polymerisation of ~ 100–200 when compared with cellulose. Chemically, it is represented by the empirical formula (C<sub>5</sub>H<sub>8</sub>O<sub>4</sub>)<sub>n</sub> that consists of 50–200 units of simple sugar residues such as *d*-glucose and *d*-galactose, among others. It typically undergoes thermal

**Table 2** Proximate properties and higher heating values (HHV) of OPEFB

MC (wt%)	VM (wt%)	AC (wt%)	FC (wt%)	HHV (MJ/kg)	References
8.75	79.67	3.02	8.65	18.96	Yang et al. [63]
7.95	83.86	5.36	10.78	19.35	Abdullah, Gerhauser [64]
8.75	79.67	3.02	8.65	**	Li et al. [65]
7.80	79.34	4.50	8.36	15.22	Lahijani, Zainal [41]
5.18	82.58	3.45	8.97	17.02	Mohammed et al. [66]
38.40	66.10	5.50	28.40	14.80	Madhiyanon et al. [34]
60.00	71.20	7.54	18.30	18.30	Langè, Pellegrini [67]
4.29	82.21	3.09	10.41	17.93	Parshetti et al. [68]
8.20	74.20	4.80	12.80	18.40	Ninduandee et al. [83]
6.80	77.4	3.30	19.30	18.10	Johari et al. [69]
5.30	75.00	7.70	17.70	20.20	Chuah et al. [72]
5.30	72.13	3.05	19.52	20.20	Shahbaz et al. [84]
32.20	67.30	5.90	26.80	20.00	Nakason et al. [73]
5.00	83.00	3.00	9.00	16.00	Ariffin et al. [31]
0.00	78.34	3.20	18.46	19.54	Hantoko et al. [74]
7.86	69.92	4.77	17.45	17.78	Yan et al. [75]
7.78	81.53	6.28	12.19	17.57	Nyakuma et al. [42]
4.55	77.42	4.19	13.84	17.57	Sukiran et al. [24]

**Fig. 2** Major components of typical biomass



decomposition or devolatilisation in a wider temperature range of 150–350 °C to generate non-condensable gases but less tar compared with cellulose [61]. This indicates that hemicellulose is more reactive than cellulose and undergoes thermal degradation more rapidly based on its lower activation at lower activation energy ( $E_a = 41\text{--}68$  kJ/mol) compared with cellulose ( $E_a = 187\text{--}235$  kJ/mol) reported in the literature [93].

The third major lignocellulose component that forms an essential part of the plant cell wall structure is lignin [94]. It typically accounts for 15–40% by weight of most plants [95]. Structurally, it is a highly branched, aromatic, or phenolic polymer comprised of monomer units of benzene-type compounds (such as phenyl propane, phenyl aniline) [95–97]. According to Sun et al. [97], lignin is the product of the oxidative coupling of *p*-coumaryl, guaiacyl, and syringyl alcoholic-based phenylpropanoid groups, which result in a highly random tri-dimensional network structure within the plant cell wall. Functionally, lignin acts as the cement, binding agent, or matrix for cellulose, thereby enhancing the structural rigidity and compressive strength to the plant cell wall [61, 98]. Similar to cellulose, lignin is largely resistant to the action of enzymatic decomposition [99, 100] due to cross-linking [97], although it is more thermally reactive ( $E_a = 97\text{--}150$  kJ/mol) than cellulose [93].

Based on the foregoing, it can be reasonably inferred that lignocellulosic composition is crucial to the process design, operational parameters, product yields, and distribution from the conversion of biomass. Hence, the lignocellulosic

composition of OPEFB has been examined by many researchers in the literature, as summarised in Table 3.

As observed, the composition of cellulose (%) for OPEFB as empirically determined by the various authors ranging from 19.06–43.80% (or an average of 33.80%), whereas hemicellulose (%) is from 13.50–47.91% (or an average of 28.75%), and lastly lignin content is 16.40–35.10% (or an average of 26.29%). The findings revealed that extractives, sugars, proteins, and ash other compounds also account for 0.00–26.73% (or an average of 11.16%) of the remaining composition.

#### 2.1.4 Calorific analysis

This is a measure of the energy content of biomass fuels expressed either as the lower (LHV, MJ/kg) or higher (HHV, MJ/kg) heating values [62]. The HHV is the amount of heat evolved from the complete combustion of a unit mass of fuel at 25 °C [79]. It is thus regarded as one of the most important properties of any potential biomass feedstock for energy applications [61]. This is due to its influence on thermal conversion, efficiency, and potential energy application [110]. Typically, the HHV of any biomass is measured by bomb calorimetry according to the ASTM standard D-2015, whereas the LHV is calculated from the HHV minus the heat of vaporisation of water [61]. Alternatively, the HHV can be calculated from the ultimate or proximate properties of any feedstock, as earlier surmised. The values of HHV for various OPEFB samples in Table 2 range from 14.80 to 20.20 MJ/kg

**Table 3** Proximate properties and higher heating values (HHV) of OPEFB

Cellulose (%)	Hemicellulose (%)	Lignin (%)	Others (%)	References
22.24	20.58	30.45	26.73	Mohammed et al. [66]
38.30	35.30	22.10	4.30	Kelly-Yong et al. [101]
28.30	36.60	35.10	0.00	Palamae et al. [102]
19.06	47.91	24.45	8.58	Rodríguez et al. [103]
39.13	23.04	34.34	3.49	Ishola et al. [104]
36.67	13.50	31.16	18.67	Isroi et al. [105]
33.25	23.24	25.83	17.68	Barlianti et al. [106]
43.80	35.00	16.40	4.80	Hamzah et al. [107]
40.40	20.20	23.10	16.30	Zakaria et al. [108]
36.83	32.11	20.00	11.06	Rashid et al. [109]

or an average of 18.06 MJ/kg, indicating it is a potentially viable bioenergy feedstock.

### 2.1.5 Metals or metal oxide analysis

This is the composition of alkali–alkali earth and metals (AAEM) elements in biomass feedstocks and ash. These elements and compounds influence the yield, product distribution, potential emissions, and operational performance of biomass feedstock during thermochemical conversion [111–114]. Consequently, the AAEM compositions in biomass ashes reportedly influence the potential selection of biomass feedstocks [115, 116] due to their profound effects on corrosion, fouling, and agglomeration of biomass conversion equipment [117–119]. The determination of the inorganic composition of biomass feedstock is thus an important characterisation technique. The metal and oxide characterisation of biomass is typically performed by x-ray fluorescence (XRF) [22, 120, 121]. Other notable techniques including energy-dispersive x-ray (EDX) spectroscopy, inductively coupled plasma-optical emission spectroscopy (ICP-OES), and atomic absorption spectroscopy (AAS) have been reported [120, 122, 123]. Table 4 presents the metal element and oxides composition of OPEFB determined by XRF as reported by various researchers.

The findings reveal that OPEFB contains various concentrations of metal oxides, namely  $\text{Al}_2\text{O}_3$ ,  $\text{CaO}$ ,  $\text{Cl}$ ,  $\text{Cr}_2\text{O}_3$ ,  $\text{CuO}$ ,  $\text{Fe}_2\text{O}_3$ ,  $\text{K}_2\text{O}$ ,  $\text{MgO}$ ,  $\text{MnO}$ ,  $\text{NiO}$ ,  $\text{P}_2\text{O}_5$ ,  $\text{Rb}_2\text{O}$ ,  $\text{SiO}_2$ ,  $\text{SO}_3$ ,  $\text{SrO}$ ,  $\text{TiO}_2$ ,  $\text{ZnO}$ , and  $\text{ZrO}_2$ . The major oxides comprised of  $\text{K}_2\text{O}$ ,  $\text{SiO}_2$ ,  $\text{CaO}$ ,  $\text{Cl}$ ,  $\text{MgO}$ ,  $\text{P}_2\text{O}_5$ ,  $\text{Fe}_2\text{O}_3$ ,  $\text{SO}_3$ ,  $\text{Al}_2\text{O}_3$ , and  $\text{Na}_2\text{O}$ , whereas  $\text{Rb}_2\text{O}$ ,  $\text{MnO}$ ,  $\text{ZnO}$ ,  $\text{TiO}_2$ ,  $\text{CuO}$ ,  $\text{SrO}$ ,  $\text{Br}$ , and  $\text{NiO}$  are typically detected in trace amounts in OPEFB. The metal oxides are known to react with silica at high temperatures thereby forming eutectic mixtures that melt in the range from 754 to 875 °C compared with 1450 °C for  $\text{SiO}_2$ . As a result, the bed materials are prone to sintering, clinker formation, and bed agglomeration that result in the formation of hot spots

and de-fluidisation. The characterised metal oxide properties of biomass can then be used to predict the behaviour of bed materials in biomass reactors [77]. Such predictions are based on empirical-based relations proposed by numerous researchers to examine fouling, sintering, and bed agglomeration based on the metal oxides [127, 128].

### 2.2 Thermal properties

The thermal characterisation of biomass feedstock offers valuable insights into the effects of temperature, heating rates, and the isothermal/non-isothermal conditions on the decomposition behaviour, stability, purity, potential products and yield during conversion. The thermal properties of biomass can be characterised by thermogravimetric analysis (TGA), differential scanning calorimetry (DSC), and derivative thermal analysis (DTA). According to the analysts [59, 129, 130], TGA is the most frequently used analytical technique for analysing the thermal properties of biomass. TGA is a high-precision and robust technique for investigating the thermal degradation, reaction mechanisms, and kinetic properties of materials [131–133]. In practice, TGA measures the mass (weight) loss of materials at specific heating rates and temperatures under either inert ( $\text{N}_2$ , Ar), oxidising (air,  $\text{O}_2$ ), or combined conditions [134, 135]. During each TGA run, the selected material is heated in either isothermal [136–138], non-isothermal, or mixed modes to examine its thermal properties [139, 140]. On completion, the resulting data is retrieved and plotted as either mass loss (TG, %) or derivative mass loss (DTG, %/min) against temperature (°C or K) or time (min or s) [141].

The TG-DTG plots are then analysed to deduce the temperature profile characteristics (TPCs) required to examine the thermal properties of materials [142, 143]. The TPCs provide insights into the thermal decomposition, degradation processes, and reaction mechanisms [129, 132]. The TPCs are determined using proprietary thermal analysis software installed

**Table 4** Metal oxide compositions of OPEFB

Metal oxide	References						
	Lahijani, Zainal [41]	Madhiyanon et al. [34]	Mohammed et al. [66]	Asadieraghi, Daud [124]	Fukuda [125]	Ninduangdee, Kuprianov [36]	Kadir et al. [126]
Na <sub>2</sub> O	0.55	0.09	1.54	0.23	0.00	0.36	0.31
MgO	4.80	1.90	8.75	3.68	2.50	3.24	4.25
Al <sub>2</sub> O <sub>3</sub>	0.97	0.26	1.22	0.77	0.40	3.11	8.27
SiO <sub>2</sub>	27.00	12.12	10.83	19.24	16.10	26.21	25.40
P <sub>2</sub> O <sub>5</sub>	3.60	0.00	1.84	4.29	6.80	1.21	0.87
SO <sub>3</sub>	2.70	1.66	0.00	0.00	0.40	0.00	7.56
Cl	5.30	6.84	5.30	0.00	4.30	2.54	0.00
K <sub>2</sub> O	44.00	55.48	53.73	39.98	53.20	47.21	7.41
CaO	8.00	9.65	12.50	15.52	12.50	12.54	13.33
TiO <sub>2</sub>	0.08	0.00	0.00	0.00	0.00	0.00	1.59
MnO	0.11	0.00	0.00	0.00	0.00	0.00	0.51
Fe <sub>2</sub> O <sub>3</sub>	3.00	0.00	3.60	5.78	3.50	3.21	15.84
NiO	0.01	0.00	0.00	0.00	0.00	0.00	0.00
CuO	0.04	0.00	0.00	0.00	0.00	0.00	0.15
ZnO	0.09	0.00	0.00	0.32	0.00	0.00	0.00
Br	0.02	0.00	0.00	0.00	0.00	0.00	0.00
Rb <sub>2</sub> O	0.12	0.00	0.00	0.00	0.00	0.00	0.00
SrO	0.03	0.00	0.00	0.00	0.00	0.00	0.00
ZrO <sub>2</sub>	Trace	0.00	0.00	0.00	0.00	0.00	0.00
BaO	0.00	0.00	0.00	0.00	0.00	0.00	0.00
PbO	Trace	0.00	0.00	0.00	0.00	0.00	0.00

during the commissioning of the TG Analysers. Conversely, the tangent method proposed in the literature by various authors can be used in place of the software [59, 63, 144]. The TPCs employed to examine and describe the effects of temperature or heating rates on the thermal decomposition are onset (ignition) temperature ( $T_i$  or  $T_{\text{onset}}$ ), maximum (peak) decomposition temperature ( $T_{\text{max}}$  or  $T_{\text{peak}}$ ), offset (burnout) temperature ( $T_{\text{end}}$ ), mass loss ( $M_L$ ), mass loss rate (MLR), and residual mass ( $R_M$ ) [60, 132].

The onset or ignition temperature ( $T_i$  or  $T_{\text{onset}}$ ), offset or burnout ( $T_{\text{end}}$ ) temperature, mass loss ( $M_L$ ), and residual mass ( $R_M$ ) are typically determined from the TG plots. The maximum or peak decomposition temperature ( $T_{\text{max}}$  or  $T_{\text{peak}}$ ), and mass loss rate (MLR) are deduced from the DTG plots.  $T_{\text{onset}}$  is a measure of the ease of thermally igniting any material during TGA. It is also defined as the temperature any material starts to devolatilise or decompose during thermal analysis.  $T_{\text{end}}$  is the final temperature of devolatilisation and typically marks the termination of the process.  $T_{\text{peak}}$  is defined as the temperature at which the maximum mass loss (%) of the sample occurs during TGA. It is typically characterised by high rates of mass loss, denoted as MLR, which is ascribed to the decomposition of volatiles (i.e. devolatilisation) and

lignocellulosic components of biomass such as hemicellulose, cellulose, and lignin [145]. The residual mass ( $R_M$  in %) is the final mass of the material remaining in the TGA crucible at the final TGA temperature [140, 143].

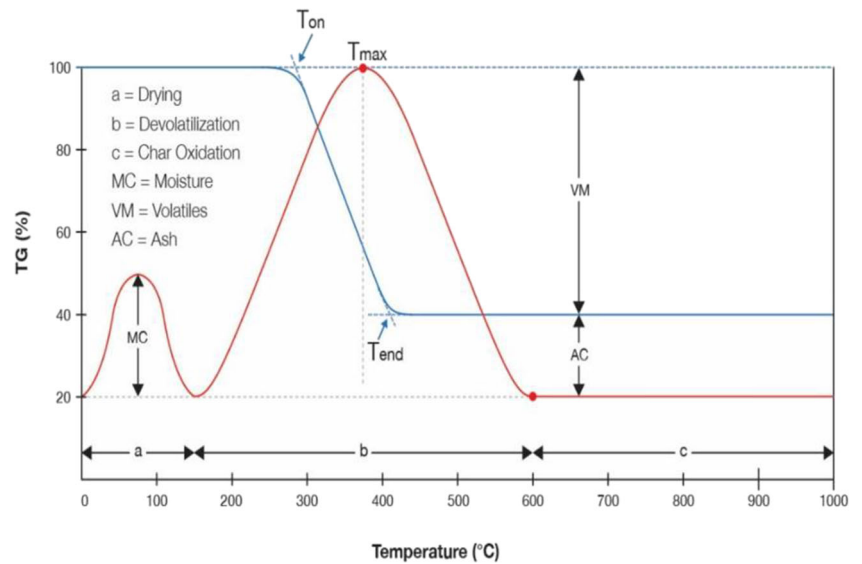
Based on the thermal properties and TPCs deduced during TGA from various studies [146–148], biomass decomposition occurs in three (3) stages, namely *a*—drying ( $< 150$  °C); *b*—actively pyrolysis ( $> 150$ – $600$  °C); and *c*—passive pyrolysis ( $> 600$  °C) as shown in Fig. 3 adapted from Cai et al. [59]. In Fig. 3, the blue line represents the thermogravimetric (TG) plot, whereas the red line denotes the derivative thermogravimetric (DTG) plot.

The mass loss during the first stage is attributed to the removal of moisture and low molecular weight volatiles [145, 147]. The second mass loss stage, known as the active stage of pyrolysis or devolatilisation, is attributed to the significant degradation of hemicellulose, cellulose, lignin, and other organic matter components during TGA [132, 145, 149]. The final stage is mainly attributed to lignin decomposition and characterised by slow rates of degradation and the tailing observed after  $600$  °C in Fig. 3 [131, 148].

Table 5 presents the different operating conditions employed to determine the thermal properties of OPEFB



**Fig. 3** TG-DTG plots and TPCs for biomass decomposition



during or after TG analysis. The key operating conditions for the thermal decomposition of OPEFB are sample mass (mg), heating rate (°C/min), purge gas, gas flow rate (mL/min), operating atmospheric conditions, TGA temperature range (°C),

and mode of heating. Furthermore, the thermal decomposition behaviour, characteristic temperature profiles, and reaction mechanisms of OPEFB decomposition have been examined from the resulting TG-DTG plots. Typically, a small mass of

**Table 5** TGA operating conditions for OPEFB decomposition

Sample mass (mg)	Heating rate (°C/min)	Purge gas	Flow rate (mL/min)	Operating atmosphere	Temperature range (°C)	Heating mode	References
20	10	Nitrogen	120	Non-oxidative	25–900	Isothermal/non-isothermal	Yan et al. [150]
10	10	Nitrogen	100	Non-oxidative	100–600	Non-isothermal	Abdullah, Gerhauser [64]
20	10–20, 40, 60	Nitrogen	150	Non-oxidative	30–900	Non-isothermal	Idris et al. [151]
10	10	Air	10	Oxidative	25–600	Non-isothermal	Omar et al. [152]
15	10	Air	10	Oxidative	25–900	Non-isothermal	Lahijani, Zainal [41]
20	10–20, 40, 60	Air	150	Oxidative	25–1100	Isothermal/non-isothermal	Idris et al. [153]
10	10, 20, 30	Nitrogen	100	Oxidative	25–1000	Isothermal/non-isothermal	Mohammed et al. [66]
7–20	10	Nitrogen	30	Non-oxidative	100–500	Non-isothermal	Izani et al. [154]
2 × 10 <sup>3</sup>	10	Nitrogen	100	Non-oxidative	25–200, 300	Isothermal/non-isothermal	Sabil et al. [155]
20	10	Nitrogen	40–60	Non-oxidative	30–600	Non-isothermal	Chowdhury et al. [156]
1 × 10 <sup>3</sup>	50, 80	Nitrogen	150	Non-oxidative	25–700	Iso-/non-isothermal	Alias et al. [157]
5.65	10	Nitrogen	20	Non-oxidative	25–900	Non-isothermal	Auta et al. [158]
5	15	Nitrogen	150	Non-oxidative	35–850	Non-isothermal	Asadieraghi, Daud [124]
10	10	Nitrogen	20	Non-oxidative	30–600	Non-isothermal	Harmaen et al. [159]
10	10	Nitrogen	100	Non-oxidative	28–1000	Non-isothermal	Mohamed, Hamzah [160]
15	10, 20, 30, 40	Air	50	Oxidative	30–900	Non-isothermal	Ninduangdee et al. [83]
10	10, 20, 30	Nitrogen	20–50	Non-oxidative	30–900	Iso-/non-isothermal	Dewayanto et al. [161]
10	10	Air	150	Non-oxidative	25–900	Non-isothermal	Novianti et al. [162]
9.5	10	Nitrogen	20	Non-oxidative	50–850	Iso-/non-isothermal	Yahaya et al. [163]
2	10, 20, 30	Nitrogen	60	Non-oxidative	25–600	Non-isothermal	Poudel et al. [164]
9	5, 10, 15, 20, 30	Nitrogen	20	Non-oxidative	25–800	Non-isothermal	Nyakuma et al. [42]

pulverised OPEFB of particle size ranging from 125 to 500  $\mu\text{m}$  is heated in various types of crucibles (alumina, platinum, aluminium) from 25 to 1100 °C at designated heating rates from 5 to 60 °C/min.

Concurrently, the furnace is purged with air or nitrogen gas at variable flow rates ranging from 10 to 150 mL/min to remove the gases released during TG analysis. Based on the findings, the potential product yield, evolved gas compositions, and decomposition behaviour of OPEFB under conditions that simulate torrefaction [155, 164, 165], pyrolysis [64, 151, 152], and combustion [41, 83, 153] have been examined comprehensively in the literature. Likewise, the TG-DTG plots from the studies present comprehensive data on the TPCs of OPEFB during thermal decomposition. Table 6 presents the TPCs; ignition ( $T_{\text{onset}}$ ), maximum or peak decomposition ( $T_{\text{peak}}$ ), and offset ( $T_{\text{end}}$ ), temperatures along with the mass loss ( $M_L$ ), mass loss rate ( $M_{LR}$ ), and residual mass ( $R_M$ ) deduced from the resulting TG-DTG plots for OPEFB.

The ignition ( $T_{\text{onset}}$ ) for OPEFB decomposition occurs from 190 to 377 °C; the peak decomposition ( $T_{\text{peak}}$ ) from 261 to 432 °C and offset ( $T_{\text{end}}$ ) from 315 to 641 °C. The mass loss ( $M_L$ ) and residual mass ( $R_M$ ) revealed that the thermal decomposition of OPEFB results in a significant mass loss under the conditions investigated. The mass loss was observed from  $M_L = 73\text{--}99.94\%$ , whereas the residual mass was in the range  $R_M = 0.06\text{--}27\%$  during the thermal decomposition of OPEFB. Furthermore, the results revealed the thermal decomposition of OPEFB occurs in three stages; drying, devolatilisation and char degradation, as earlier illustrated in Fig. 3. For OPEFB, the drying stage of thermal decomposition typically occurred below 150 °C, whereas the devolatilisation or active pyrolysis stage was between 150 and 650 °C, and the char degradation or passive pyrolysis due to lignin

decomposition occurred above 650 °C. The results are thus in good agreement with other biomass reported in the literature [146–148]. The thermal analysis of biomass is a precursor test for examining its kinetic properties such as the activation energy ( $E_a$ ), pre-exponential or frequency factor ( $A$ , or  $k_o$ ) and reaction order ( $n$ ) [129, 166]. The review of literature on the fundamental theories, assumptions, and model equations employed to characterise and examine the kinetic properties of potential biomass in literature are presented next.

## 2.3 Kinetic properties

The kinetic properties of biomass provide valuable insights into the reaction rates and energy required for thermochemical conversion [166, 167]. Table 7 presents examples of the models commonly adopted to examine the kinetics of biomass in the literature [168, 169].

Typically, kinetic analyses are adopted to critically examine the effects of temperature and heating rate on the thermochemical conversion process [132, 133]. Various kinetic models, theories, and techniques have been proposed to perform kinetic analysis and elucidate the specific kinetic properties of biomass undergoing thermochemical conversion [170]. Broadly, there are two major approaches for analysing the kinetic parameters of biomass decomposition, namely model-fitting, and model-free or *isoconversional* methods [129, 133].

### 2.3.1 Model fitting

These methods are used to determine the kinetic parameters of materials by first defining the best statistical fit from the TGA data [129]. The advantage of the method is its ability to

**Table 6** Characteristic temperature profiles (TPCs) for OPEFB

Drying range (°C)	Devolatilisation range (°C)	DTG peaks	$T_{\text{onset}}$ (°C)	$T_{\text{peak}}$ (°C)	$T_{\text{end}}$ (°C)	Residual mass ( $R_M$ , %)	Mass loss ( $M_L$ , %)	References
< 250	250–380	2	285	355	375	5.43	94.57	Abdullah, Gerhauser [64]
< 150	350–500	2	200	432	-	0.06	99.94	Idris et al. [151]
< 150	175–550	3	190	315	-	6.00	94.00	Omar et al. [152]
< 100	220–460	3	200–250	268	400–425	5.80	94.20	Lahijani, Zainal [41]
< 150	200–550	3	377	396	-	3.57	96.43	Idris et al. [153]
< 150	200–600	3	170–187	270–303	489–616	-	-	Mohammed et al. [66]
< 150	200–400	2	237	261	315	27.00	73.00	Izani et al. [154]
< 150	200–420	2	-	329	-	14.50	85.50	Asadieraghi, Daud [124]
< 150	200–400	2	200–220	337	375–425	-	-	Mohamed, Hamzah [160]
< 150	200–650	3	258–280	277–319	504–641	-	-	Ninduangdee et al. [83]
< 150	150–380	3	-	308	-	8.77	91.23	Yahaya et al. [163]
< 150	252–368	2	252–276	302–327	332–368	19.64–25.82	74.18–80.36	Nyakuma et al. [42]

**Table 7** Methods for examining biomass decomposition kinetics

Kinetic model	Approach	Examples
Model fitting	Conventional (isothermal)	Differential, Freeman–Carrol (FCM), Horowitz–Metzger (HMM), Coats–Redfern model (CRM).
Model free ( <i>isoconversional</i> )	Standard (non-isothermal)	Kissinger model (KSM), Starink model (STK), Kissinger–Akahira–Sunose (KAS), Flynn–Wall–Ozawa (FWO).

determine kinetic parameters based on a single TGA experiment, which saves time, costs, and materials [149, 169]. The major drawback is that forehand knowledge and appropriate selection of the reaction model is required before analysis of the kinetic properties [171]. Another drawback is that the model fitting methods produce similar conclusions since any function of conversion can suitably fit experimental data at the expense of accurately determining the kinetic parameters [172]. As a result, the kinetic parameters calculated from model fitting models tend to differ significantly from isoconversional model values as reported in the literature [129, 173]. The most common examples of model-fitting models adopted by researchers include the Freeman–Carrol, Horowitz–Metzger, and Coats–Redfern (CR). The CR method is the most widely adopted model-fitting model, and as such, it has been extensively applied to examine the kinetics of biomass conversion [145, 174–177]. The governing equation for the kinetic parameter analysis from the CR method is presented as

$$\ln \left[ \frac{-\ln(1-\alpha)}{T^2} \right] = \ln \left[ \frac{AR}{\beta E_\alpha} \left( 1 - \frac{2RT}{E} \right) \right] - \frac{E_\alpha}{RT} \quad (3)$$

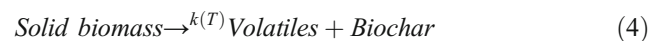
The expression used to describe the rate of biomass decomposition at a constant heating rate is given as  $\beta = \frac{dT}{dt}$ . By plotting  $\ln \left[ \frac{-\ln(1-\alpha)}{T^2} \right]$  against  $\frac{1}{T}$ , a straight line can be obtained from which the activation energy ( $E_\alpha$ ) and the frequency factor ( $A$ ) can be deduced from the slope,  $-\frac{E_\alpha}{R}$  and  $\ln \left[ \frac{AR}{\beta E_\alpha} \right]$  respectively.

### 2.3.2 Model-free (isoconversional)

These models are simpler, error-free, and more reliable methods for determining the kinetic properties of biomass based on multiple heating rates adopted during TGA. The models can thus be applied without knowledge of the reaction mechanisms involved in the process, as required by the model fitting models [171, 178]. The uncertainties encountered while estimating kinetic properties from model-fitting can thus be

avoided by adopting the isoconversional methods [133, 172]. The challenge of the model-free approach is that it is not only expensive and time-consuming but requires more quantities of materials for TG analysis. Nonetheless, the isoconversional methods provide a compromise to the oversimplified single-step Arrhenius kinetic treatments [166] or the model-fitting approach. Over the years, the models have been successfully applied to examine the thermal decomposition kinetics of a wide variety of biomass, namely wood chips [147], corn cobs [149], cardoon (*Cynara cardunculus*) [130], orange wastes [148], hazelnut husks [132], blooming-forming cyanobacteria [179]; *Imperata cylindrica* grass [60], red pepper waste [166], biochar [138], and waste sawdust [180]. The most commonly applied kinetic models for estimating the kinetic properties are Flynn–Wall–Ozawa (FWO), Kissinger (KSM), and Kissinger–Akahira–Sunose (KAS) models [181–183]. Other notable models including Friedmann [184], Starink [185], Vyazovkin [186], Cai–Chen [187], and the Distributed Activation Energy Model (DAEM) [188] are also reported in the literature.

In principle, the isoconversional models are developed from the one-step global theory of solid-state decomposition. The theory assumes that the thermal decomposition of any solid material can be described by first-order reactions based on the relation [166, 189]:



Based on this relation, the decomposition of biomass typically yields volatiles that consist of gases and liquid or tar, along with biochar. The yield and composition of products are influenced by the temperature-dependent rate constant  $k(T)$  described as

$$k(T) = A \exp \left( -\frac{E_\alpha}{RT} \right) \quad (5)$$

The terms  $k(T)$  represent the temperature-dependent rate constant;  $A$ —frequency factor ( $\text{min}^{-1}$ ) at the degree of conversion ( $\alpha$ );  $E_\alpha$ —activation energy (kJ/mol) at the degree of

conversion ( $\alpha$ );  $R$ —molar or ideal gas constant (J/mol K);  $T$ —temperature (K) at the degree of conversion ( $\alpha$ ). The rate of biomass conversion into volatiles and biochar is given as

$$\frac{d\alpha}{dt} = k(T)f(\alpha) \quad (6)$$

where the term  $f(\alpha)$  represents the reaction model at various degrees of biomass conversion. Based on the selected isoconversional method, the degree of conversion ( $\alpha$ ) of thermal decomposing material is expressed as [179]

$$\alpha = \frac{m_i - m_a}{m_i - m_f} \quad (7)$$

where the terms  $m_i$ —initial mass of the sample;  $m_a$ —actual mass of the sample; and  $m_f$ —final mass of the sample. Thus, the degree of conversion ( $\alpha$ ) can be deduced from the relation [129, 190]

$$\frac{d\alpha}{dt} = A \exp\left(-\frac{E_\alpha}{RT}\right) f(\alpha) \quad (8)$$

Equation 8 is the fundamental governing equation for the kinetic methods (models) used to examine biomass decomposition. By applying the modified Arrhenius equation (Eq. 5), an expression for the function  $f(\alpha)$  and its derivative  $(1 - \alpha)^n$  can be applied to describe biomass conversion at the selected heating rate ( $\beta$ ) based on the expression

$$\frac{d\alpha}{dT} = \frac{A}{\beta} \exp\left(-\frac{E_\alpha}{RT}\right) (1 - \alpha)^n \quad (9)$$

After the separation of variables, the integral that describes the thermally decomposing materials can be expressed as

$$g(\alpha) = \int_0^\alpha \frac{d\alpha}{(1 - \alpha)^n} = \frac{A}{\beta} \int_{T_0}^T \exp\left(-\frac{E_\alpha}{RT}\right) dT \quad (10)$$

Based on Eq. 10, the isoconversional models of Flynn–Wall–Ozawa (FWO) and Kissinger–Akahira–Sunose (KAS) methods could be applied to the TGA data to determine the kinetic parameters for decomposition.

The FWO and KAS methods, as earlier stated, are the most commonly applied isoconversional models used to determine the kinetic parameters activation energy,  $E_\alpha$ , and frequency factor,  $A$ . The FWO method is defined by the expression [181, 182]

$$\ln(\beta) = \ln\left(\frac{A_\alpha E_\alpha}{R_g(\alpha)}\right) - 5.331 - 1.052 \frac{E_\alpha}{RT_{\alpha i}} \quad (11)$$

The kinetic parameters  $E_\alpha$  and  $A$  can be thus determined by plotting  $\ln(\beta)$  against  $1/T$ , where the slope is defined by  $-1.052 E_\alpha/R$  for the FWO method. The KAS method was derived from the original Kissinger model [183, 191]:

$$\ln\left(\frac{\beta}{T_m^2}\right) = \ln\left(\frac{A_\alpha R}{E_\alpha}\right) - \frac{E_\alpha}{RT_{\alpha i}} \quad (12)$$

The maximum peak decomposition temperature  $T_m$  can be substituting for  $T$  in Eq. 12 to account for conversion ( $\alpha$ ) during TGA, to obtain the KAS model expressed as

$$\ln\left(\frac{\beta}{T^2}\right) = \ln\left(\frac{A_\alpha R}{E_\alpha g(\alpha)}\right) - \frac{E_\alpha}{RT_{\alpha i}} \quad (13)$$

The terms  $\beta$  represent the heating rate ( $^\circ\text{C}/\text{min}$ );  $g(\alpha)$ —fractional conversion of the biomass;  $A_\alpha$ —frequency factor at the degree of conversion ( $\alpha$ ) ( $\text{min}^{-1}$ );  $E_\alpha$ —activation energy at  $\alpha$  (kJ/mol);  $T_{\alpha i}$ —temperature at  $\alpha$  (K); and  $R$ —molar gas constant (J/mol K). Similarly, by plotting  $\ln(\beta/T^2)$  vs  $1/T$  or  $\ln(\beta/T_m^2)$  vs  $1/T_m$  using the KAS and Kissinger methods respectively, the kinetic parameters can also be obtained. The frequency factor ( $A$ ,  $\text{min}^{-1}$ ) is determined from the intercepts of the FWO and KAS plots. The values of  $A$  and reaction order ( $n$ ) can also be computed from the Coats–Redfern method [130]. The values of  $A$  can be computed from the correlation between the intercept and  $\ln(AR/\beta E_\alpha)$  based on the assumption that  $2RT \ll E_\alpha$ . The flexibility of the described models ensures that the kinetic properties of materials undergoing thermal decomposition can be determined from isoconversional data. Based on the foregoing, the kinetic properties of OPEFB decomposition have been examined by several researchers in the literature.

Table 8 presents a review of literature on the kinetic parameters activation energy ( $E_a$ ,  $\text{kJ mol}^{-1}$ ) and frequency factor ( $A$ ,  $\text{min}^{-1}$ ) properties of OPEFB. Table 8 also shows that the kinetic analyses of OPEFB under torrefaction [164], pyrolysis [151], and combustion [83, 153] conditions were successfully examined by TGA. The studies were extended to compute the activation energy ( $E_a$ ), and frequency factors ( $A$ ) values through model-fitting and model-free models. The results showed that under non-oxidative conditions, the  $E_a$  for OPEFB was between 37.85 and 209.68 kJ/mol (or 123.77 kJ/mol on average), which is significantly higher than the oxidative process with  $E_a$  values that ranged from 68.90 to 105.56 kJ/mol (or 83.09 kJ/mol on average). Likewise, the frequency factor ( $A$ ) under non-oxidative conditions was from  $3.95 \times 10^{07} \text{ min}^{-1}$  to  $1.45 \times 10^{17} \text{ min}^{-1}$  (or  $7.25 \times 10^{16} \text{ min}^{-1}$  on average), whereas the values were between  $4.86 \times 10^{08} \text{ min}^{-1}$  and  $7.50 \times 10^{10} \text{ min}^{-1}$  (or  $2.73 \times 10^{10} \text{ min}^{-1}$  on average) for the oxidative process. Although the kinetic parameters were obtained at high regression coefficients (90–99%), the thermochemical conversion of OPEFB under oxidative conditions occurred more rapidly compared with non-oxidative conditions. Based on the lower values of  $E_a$  and  $A$ , the plausible inference is that the OPEFB particles acquired sufficiently higher thermal energy due to the exothermic nature to undergo rapid degradation compared with the process

**Table 8** Kinetic parameters for OPEFB decomposition

Heating rate (°C/min)	Start and end TGA temp. (°C)	$E_a$ (kJ mol <sup>-1</sup> )	A (min <sup>-1</sup> )	$R^2$	Kinetic models	References
10, 20, 40, 60	30–900	209.68	$1.45 \times 10^{17}$	0.99	Kissinger	Idris et al. [151]
10, 20, 40, 60	25–1100	105.56	**	**	Flynn–Wall–Ozawa (FWO)	Idris et al. [153]
10, 20, 30, 40	30–900	68.90–84.70	$3.95 \times 10^{07}$ – $7.50 \times 10^{10}$	0.95–0.98	Coats–Redfern (CRM)	Ninduangdee et al. [83]
10, 20, 30	30–900	37.85	$3.95 \times 10^{07}$	0.97	Coats–Redfern (CRM)	Dewayanto et al. [161]
10, 20, 30	25–600	97.6	**	**	Coats–Redfern (CRM)	Poudeh et al. [164]
5, 10, 15, 20, 30	30–800	144.30–146.63	$2.42 \times 10^{17}$ – $5.22 \times 10^{13}$	0.90–0.91	Flynn–Wall–Ozawa (FWO) and Kissinger Akahira Sunose (KAS)	Nyakuma et al. [42]

under non-oxidative conditions. Other factors such as the enthalpy, entropy, and Gibb's free energy of the thermal degradation particles may also influence the process. Hence, thermodynamic properties of the thermally degrading particles have also been examined in the literature, as described in the subsequent section.

## 2.4 Thermodynamic properties

The thermodynamic properties present critical insights into the extent of the conversion process and the energy requirements, the heat of formation, reaction mechanisms, degradation behaviour, and state of equilibrium of biomass during thermochemical conversion [82, 166]. These outlined parameters influence the process design, engineering economics, risk safety, product selectivity, and environmentally friendly conversion of biomass [192–195]. Typically, the thermodynamic properties comprise the enthalpy, Gibb's free energy, and entropy change of biomass [195–197]. Studies by Xu et al. [196], Kim et al. [198], Vasiliu et al. [195], Maia, de Moraes [166], Kaur et al. [197] have highlighted the importance of enthalpy, Gibb's free energy, and entropy change during thermochemical conversion of biomass in chemical reactors. The enthalpy ( $\Delta H$ ) is defined as the total heat content or energy consumed during thermochemical biomass conversion into its constituent products [197]. The Gibb's free energy ( $\Delta G$ ), on the other hand, is the total energy of the system required to form the activated complex [198–200]. The entropy change ( $\Delta S$ ) is the degree of disorderliness of a system or the measure of the bond dissociation and state of equilibrium of the reacting species [197]. The enthalpy ( $\Delta H$ ), Gibb's free energy ( $\Delta G$ ), and entropy change ( $\Delta S$ ) are computed from the following mathematical expressions:

$$\text{Enthalpy } \Delta H = E_a - RT \quad (14)$$

$$\text{Gibb's free energy } \Delta G = E_a + RT_{peak} \ln \left( \frac{K_B T_{peak}}{hA} \right) \quad (15)$$

$$\text{Entropy } \Delta S = \frac{\Delta H - \Delta G}{T_{peak}} \quad (16)$$

The term  $\Delta H$  denotes the enthalpy (kJ/mol);  $\Delta G$  is Gibb's free energy (kJ/mol);  $\Delta S$  is the entropy change (J/mol); and  $T_{peak}$  is the peak decomposition temperature (°C) deduced from the DTG plots. The symbol  $K_B$  represents the Boltzmann's constant ( $1.38 \times 10^{-23}$ , J/K), whereas  $h$  is Planck's constant ( $6.626 \times 10^{-34}$ , Js).

Kaur et al. (2018) investigated the thermodynamic properties of castor residues from the activation energy  $E_a$  and pre-exponential factor  $A$  based on the isoconversional models of FWO and KAS. The findings showed that the enthalpy ( $\Delta H$ ) fluctuated from 160.91 to 162.15 kJ/mol, whereas its Gibb's free energy ( $\Delta G$ ) was between 152.05 and 152.11 kJ/mol. Maia and de Moraes (2016) examined the thermodynamic properties of red pepper wastes (RPW). The authors reported that the enthalpy ( $\Delta H$ ) of RPW varied between 23.37 and 142.21 kJ/mol; Gibb's free energy ( $\Delta G$ ) was from 71.77 and 207.03 kJ/mol, and entropy ( $\Delta S$ ) was between  $-8.31$  and  $-249.52$  J/mol. The findings of Maia and de Moraes (2016) were found to be consistent with rice husk-based composites [199], rice straw, rice bran, and chicken manure [201]. The thermodynamic properties of pelletised OPEFB have been reported for the non-oxidative thermal decomposition of the OPEFB in literature [42]. The values of  $\Delta H$ ,  $\Delta G$ , and  $\Delta S$  were calculated from the  $E_a$  and  $A$  based on the FWO model. The findings revealed that the enthalpy ( $\Delta H$ ) was from 79.05 to 190.57 kJ/mol, whereas Gibb's free energy ( $\Delta G$ ) was between 298.71 and 538.59 kJ/mol. The change in entropy ( $\Delta S$ ) ranged from  $-348.02$  to  $-219.65$  J/mol. Based on the reviewed studies, the thermodynamic properties of biomass bear correlation with the kinetic properties, decomposition mechanics, equilibrium state, and thermal reactivity during thermochemical conversion. Babu, Chaurasia [192] also demonstrated a correlation between particle size and thermodynamic properties. For large-sized particles of biomass in a thermally thick regime, the conversion time increases with an increase in the thermal conductivity. Ultimately, this yields

high char at the expense of gaseous products from the reactor. Based on its thermodynamic properties, Nyakuma et al. [42] reported that OPEFB pellets experienced rapid thermal decomposition, shorter reaction times, and the formation of an activated or intermediate complex. Drescher, Brüggemann [193] observed that the thermodynamic properties of biomass are critical to the design and operation of an organic Rankine cycle (ORC) power plants. The study also observed that thermal efficiency and total heat efficiency are the most critical variables for the biomass plant design and operation. The authors opined that it is critical to examine the thermodynamic properties of biomass feedstock prior to reactor design and thermochemical conversion.

### 3 Pre-treatment methods

This section presents the various pre-treatment techniques typically adopted to enhance the fuel properties of potential biomass feedstocks such as OPEFB. The pre-treatment techniques, namely drying, pulverisation, and pelletisation, typically adopted to process potential biomass such as OPEFB before conversion, storage, or transport are highlighted hereafter. Figure 4 presents the schematic for the drying, size reduction, and pelletisation of OPEFB.

#### 3.1 Drying technique

This is a pre-treatment process that involves the reduction or removal of moisture from freshly harvested, raw (or green) biomass [203]. Typically, moisture exists as either surface or inherent or moisture that is stored in the interstitial spaces in the dead cells and cell wall structure of biomass. The moisture content of raw biomass is usually expressed as a percentage of the overall mass of the biomass and typically varies from 25 to 90% for non-woody or algae species [58] and 40 to 70% for woody species [110]. For oil palm wastes such as OPEFB, the as-received moisture content is usually from 38 to 70% [67, 204–206]. Such high moisture content exceeding 50% presents major challenges during the thermal conversion of biomass into bioenergy. Consequently, this necessitates pre-treatment through the process of drying due to its critical importance to the heating value and conversion efficiency [206, 207].

The direct firing of high moisture content biomass substantially increases the energy requirements for conversion particularly drying. The surface moisture of biomass must be below 10% to ensure effective energy management and conversion efficiencies [208]. In practice, the raw or freshly harvested biomass is heated above 100 °C (or below 150 °C) to reduce or remove the biomass moisture with the aid of external heaters, hot flue gases [61, 77], or waste heat [209, 210]. The drying process accounts for 15% of the energy used

during the pre-treatment of biomass for energy and industrial applications [210, 211]. In context, a total of 3.8 MJ of thermal energy is required to vaporise 1 kg of moisture and ignite biomass during gasification [61].

The process of drying, also termed dehydration, has a significant impact on the selection of a biomass conversion process, product yield, and distribution of biofuels. Svoboda et al. [212] stated that high moisture negatively affects the operation of biomass boilers, lowers burning stability, and typically generates large carbon monoxide (CO) and volatile organic component (VOC) emissions. The formation of CO and VOC is caused by high moisture content, which also results in low flame temperatures and incomplete combustion [213]. Likewise, the gasification of high moisture biomass is also prone to operation problems such as low calorific value fuel gas and high content of tar compounds [212, 214]. Hence, the drying of biomass before gasification and combustion can significantly increase conversion efficiency, operations, and reduce flue gas emissions during operation [210].

Since moisture content is empirically related to the bulk density and heating value [110], the drying process enhances the physical, chemical, thermal, and calorific properties of biomass. Ståhl et al. [215] observed that the process of drying sawdust lowered its moisture and volatile hydrocarbons, thereby improving its pelletisation potential, energy content, and application. Jewiarz et al. [216] demonstrated that optimal drying alters the fuel properties of biomass such as grindability along with particle size distribution and bulk density. Furthermore, the drying of biomass is also an important requirement for the production of pellets [212, 217]. Lastly, the storage, handling and transport of biomass feedstock are also greatly enhanced by drying.

The drying of OPEFB has been examined by various researchers in the literature using various innovative technologies such as superheated steam, fluidised bed reactors, and hybrid systems comprising solar–thermal technologies to lower its moisture content and improve its fuel properties. According to Ng et al. [202], the drying of OPEFB is accomplished through hot air and steam drying to produce long and short dried fibres, which could be used as fuels for combustion and gasification in flue gas and syngas fuels, respectively. Han et al. [206] examined the use of a hot air dryer to simulate the drying of OPEFB and enhance its fuel potential firing in biomass boilers. The results showed that the process reduced the moisture content of OPEFB from 60% in as-received basis to 20% with the optimal conditions of 23 min, the ratio of steam circulation of 0.25 and ~ 5.5% reduction in the cost of drying. The findings also showed that drying increased the heating value and efficiency of the boiler.

Hasibuan, Daud [218] examined the drying of OPEFB using superheated steam (SHS) operating at the temperatures (122 to 152 °C,  $\Delta 10$  °C), pressure (1 atm), steam velocities (0.6 to 1.2) m s<sup>-1</sup>, and moisture content (1.8 to 2.3 g). The use

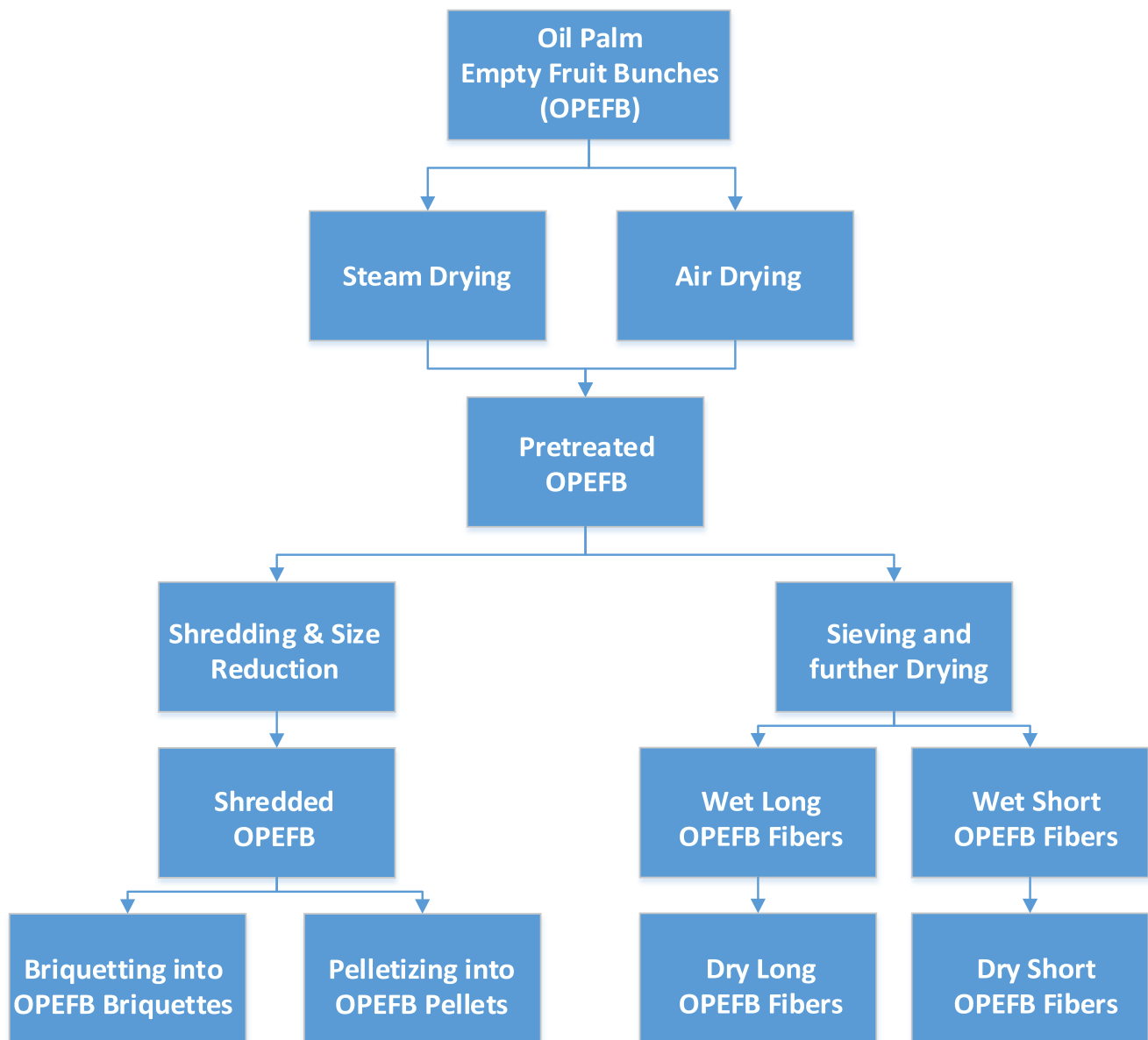


**Fig. 4** Schematic diagram for OPEFB pre-treatments (adapted from Ng et al. [202])

of SHS produces high-quality dry OPEFB, which is devoid of the problems of browning, over-drying, and dust explosion risks typically associated with hot exhaust gases and rotary drum dryers. Lastly, the authors reported that the two-stage (increasing drying rate period and falling drying rate) drying process did not affect the mechanical properties (elastic modulus and strength) of the dried OPEFB fibres. Another advantage of SHS, as reported in Svoboda et al. [212], is that it presents opportunities for rapid and high-temperature drying of small and or large particles below 15%.

In a different study, Hasibuan, Wan Daud [219] investigated the SHS drying of OPEFB at temperatures of 135 to 200 °C and steam superficial velocities (0.30 to 0.49 m/s). The effect of SHS parameters showed that the colour of the dried OPEFB was not adversely affected, whereas the microstructure was

enhanced by the removal of silica particles. In contrast, the SHS drying process caused cracks or splits in the microstructure of the dried OPEFB. The drying of OPEFB using fluidised bed has also been examined in the literature [220]. Based on the exergy recovery and energy efficiency calculations, the drying of OPEFB with a fluidised bed is an efficient process with the potential to recover and recirculate over 90% of the energy utilised during the process.

Other innovative approaches for drying OPEFB include hybrid solar-biomass thermal systems as reported in the literature [221]. The study by Al-Kayiem, Yunus [221] showed that the use of the hybrid mixed-mode solar and biomass burner drying system is a technically and economically practical approach for drying OPEFB. The findings also showed that the drying time for OPEFB was 24–32 h using the hybrid

solar–thermal dryer when compared with 52–80 h for standalone solar and 100 h for open-air sun drying. Hence, the hybrid system is more efficient compared with the standalone methods of solar, sun drying, and thermal examined in the study. In general, the reviewed literature shows that drying is an important pre-treatment process that not only reduces the moisture content of OPEFB biomass but also enhances the physical (microstructure), thermal/calorific (heating value), and operational efficiency of conversion.

### 3.2 Size reduction techniques

This is a critical physical pre-treatment process that involves the mechanical fractionation or breakdown of large biomass into small manageable sizes for effective handling, storage, transport, or conversion. Since raw biomass is harvested in a bulky or heterogeneous form, its direct conversion into biofuels, bioenergy, or biomaterials requires pre-treatment by size reduction. Typically, size reduction that occurs through grinding, pulverising, chipping, and chunking are the four (4) major classifications of size and equipment requirements, as shown in Table 9 [222].

Typically, the process begins with the mechanical disintegration or fragmentation of the large fractions of raw biomass into large chunks, which are further broken down into uniformly sized fractions called chips. Finally, the chips are then pulverised, ground, or milled using various types of dry millers [58], the most common of which is the knife and hammer grinding system [216]. In principle, the objective of size reduction is to decrease the crystallinity of the lignocellulosic fibres and minimize the heat and mass transfer limitations during conversion [223]. In addition, the bulk density, surface area, particle size distribution, and overall quality of biomass particles are improved by size reduction, which enhances automated storage, feeding, and thermal conversion [216, 224]. The process also improves the conversion efficiencies [61], as well as other pre-treatments such as drying and pelletisation of biomass. Consequently, the shelf life, transport, and storage of biomass are also greatly enhanced. The chipping and milling (grinding) of biomass into particle sizes of 10–30 mm and 0.2–2 mm [223], respectively, also enhance the specialised processing of biomass into microcrystalline cellulose, nanocellulose, and cellulose nanofibers through ball milling

[225, 226]. Typically, the process of ball milling is a specialised size reduction technique that mechanically breaks down biomass into particle sizes below 90  $\mu\text{m}$  [223], thereby decreasing the crystallinity of cellulose [227, 228].

The effectiveness of the mechanical disintegration depends on various operational and design factors such as surface area, operating load, selected equipment, and processing method of breaking down the biomass [216, 224]. Furthermore, the energy required for size reduction is usually dependent on the moisture content, particle size required, material properties, and feed rate during processing [229]. Bergman et al. [230] on the energy consumption required for grinding dry and moist poplar showed that grinding oven-dry wood expended 50–150 kWh/ton when compared with 100–325 kWh/ton for wood chips. Due to its widely reported problematic nature, several studies have been performed to improve the poor fuel properties of OPEFB through size reduction pre-treatments such as shredding, cutting, and crushing [231, 232]. Typically, shredder or shredding press machines (with the capacity of 6–8 MT/h) are employed to break, squeeze, and shred the bulky, heterogeneous, and high moisture content OPEFB into short fibres [233, 234]. The breaking process aims to mechanically disintegrate the OPEFB into sizes between 20 and 40 mm. Next, the materials are shredded into OPEFB fibres below 20 mm before squeezing (pressing) to remove residual oil and water. Lastly, the resulting fibres could then be utilised directly for biomass conversion or further ground into finer particle sizes using hammer mills for various other applications such as pelletisation or briquetting.

### 3.3 Pelletisation technique

This is the physicochemical and mechanical process of compacting or compressing loose particles of biomass into a solid uniform cylindrical structure called pellets [235]. The process of pelletisation transforms biomass particles into an energy-dense, uniformly defined, quality, and durable biofuel for various applications [236]. The pelletisation of particles significantly improves the quality, handling, storage, and supply chain of the biomass [237–239]. Traditionally, the major source of pellets is wood sawdust or timber or forestry wastes. However, the soaring demand for renewable fuels over the

**Table 9** Biomass size reduction processes and properties [222]

Process	Final products	Particle sizes	Bulk density (kg/m <sup>3</sup> )	Size (% of original)	Equipment
Pulverisation	Sawdust	< 100 $\mu\text{m}$	600	60	Pulveriser, miller
Grinding	Shavings	< 80 mm	200	20	Hammer miller
Chipping	Chips	5–50 mm	400	40	Disc/drum, chippers
Chunking	Chunks	50–250 mm	500	50	Spiral chucker



years has necessitated the pelletisation of non-traditional biomass sources such as agricultural residues [236].

The process of pelletizing biomass begins with the pre-treatment (or modification) of the selected streams of heterogeneous feedstock materials through sorting, drying, size reduction, and sieving into various particle sizes [212, 235]. Consequently, the powdered biomass particles are compacted or compressed into pellets using a pellet mill or press machine. The pellets typically with a diameter of  $D < 25$  mm are formed by the backpressure caused by the friction between the feedstock and the channel walls in the pellet mill [236]. The sizes of the channels in the matrix play an important role in determining the dimensions of the pellets, although the definite size can be optimised for each biomass pelletised. Table 10 presents the standard specifications of pellets based on the European Union STN EN 14961-2 Standard in the literature [235].

It is important to state that other national standards such as the O-NORM M7135 (Austria), SS187120 (Norway), DIN51731/DIN Plus (Germany), CTIR (Italy), Agro/Agro+ (France), and British standards are also used to test the quality, class, and durability biomass pellets based on various physical, chemical, and mechanical parameters, as outlined in Table 11 [240]. The data on the various protocols highlight the stringent standards for regulating the production, storage, or use of wood pellets for various applications. However, the French Agro/Agro+ standards are designed specifically for pellets produced from agricultural materials and hence could play a critical role in the transition from wood-based pellets to agricultural residue-based pellets in the near future.

The quality of the final biomass pellets is largely dependent on the material, structural, and technical parameters. For example, the chemical composition (moisture, ash, and lignocellulosic content), fractional size, additives (binder) materials, and density of the feedstock biomass are crucial to pellet quality [241, 242]. The quality of biomass pellets is also influenced by the pressing pressure, compaction temperature, speed, and residence time and selected unit operations for pelletisation [243, 244]. Other technical parameters such as

the dimensions of the matrix (length and radius of the channel), coefficient of sliding friction, and elastic modulus and Poisson's ratio of the biomass also influence the final quality of the pellets [236]. Despite the numerous quality standards and manufacturing guidelines, pellets are prone to mechanically induced wear and tear during handling, which results in fine dust (FD) or particulate matter (PM) production. The presence of PM/FD presents significant risks to human health, safety owing to fires, explosions, and hazards [240]. Despite the outlined challenges, pelletisation is a practical approach for pre-treating biomass and improving its fuel quality for various applications.

Numerous studies have investigated the effect of pelletisation on the thermochemical conversions of agricultural wastes, forestry wastes, and biodiesel wastes [245–249]. Other researchers investigated the effects of pelletisation on the fuel properties and energy conversion of oil palm wastes (OPW) [250–253]. Rahman et al. [251] examined the power generation potential of OPEFB pellets produced with a sago starch binder. Pelletisation improved the durability, solid form, and bulk density of OPEFB, although the calorific value, moisture, and ash content of the pellets were adversely affected due to the sago starch-binding agent. The binder also enhanced the durability of the pellets by reducing breakage, particulates, and loose fibres in pelletised OPEFB under low compression pressures [251]. Nasrin et al. [254] examined the process of pelletizing OPEFB in a typical palm oil mill. The study examined the effect of OPEFB and PKS blend ratios of 20, 30, 40, and 60% on the calorific values, density, and durability of pellets. The results demonstrated that the pelletised OPWs exhibited improved calorific fuel properties, lower moisture, and ash contents compared with raw OPEFB. In summary, the studies reviewed highlight the prospects and benefits of characterising and pre-treating biomass feedstocks such as OPEFB. Although the quality of characterised and pre-treated biomass is superior to the raw or harvested versions, the processes are considered expensive and energy-intensive, which could significantly influence the techno-economic aspect of biomass pre-treatment and conversion. The next section comprehensively reviews other significant challenges associated with biomass characterisation and pre-treatment techniques with emphasis on OPEFB in the literature.

**Table 10** Pellet specifications based on STN EN14961-2 standard [235]

Code	Dimensions in mm		
	Diameter	Minimum length	Maximum length
D06	6 ± 1.00	3.15	40
D08	8 ± 1.00	3.15	40
D10	10 ± 1.00	3.15	40
D12	12 ± 1.00	3.15	50
D25	25 ± 1.00	10.00	50

## 4 Challenges of characterisation and pre-treatment

The direct utilisation of raw or freshly harvested biomass is problematic due to their numerous heterogeneous fuel properties. The OPEFB generated from the extraction of CPO in palm oil mills is characterised by high moisture (> 60%), ash, mineral matter, metal oxides, and extraneous materials

**Table 11** Wood pellet quality standard and values based on European standards [240]

Norm of pellets	DIN 51 731	ONORM M7135	DINplus	EN 14961	Agro+	Agro
Diameter (mm)	4–10	4–10	**	6–25	6–8	6–16
Length (mm)	≤ 50	< 5*d	< 5*d	3.15–50	10–30	10–30
Abrasion (%)	**	≤ 2.3	≤ 2.3	≤ 1–3	≤ 5	≤ 8
Heating value (MJ/kg)	17.5–19.5	> 18	> 18	≥ 13.2–19	≥ 15.5	≥ 14.7
Water content (%)	≤ 12	≤ 10	≤ 10	≤ 10–15	≤ 11	≤ 15
Ash content (%)	< 1.5	< 0.5	< 0.5	≤ 3–10	≤ 5	≤ 7
Density (kg/m <sup>3</sup> )	> 540	> 540	> 540	≥ 600	≥ 650	≥ 650
Additives (%)	Not allowed	≤ 2	≤ 2	≤ 2–5	No limit	No limit
S (%)	< 0.08	< 0.04	< 0.04	≤ 0.04–0.2	≤ 0.2	≤ 0.2
N (%)	< 0.3	< 0.3	< 0.3	≤ 1–2	≤ 1.5	≤ 2
Cl (%)	< 0.03	< 0.02	< 0.02	< 0.03–0.3	< 0.2	< 0.3

along with its bulky and heterogeneous nature. The high moisture and heterogeneous nature of OPEFB account for its low calorific value, energy density, bulk density, and poor grindability. The moist, bulky, heterogeneous, and fibrous nature of OPEFB could result in deposition, blockage, self-ignition, and safety risks [255, 256]. The outlined properties also hamper effective collection, handling, storage, and transport. Furthermore, the presence of extraneous materials affects the conversion efficiency, equipment lifespan, and operating costs. The high ash and metal oxide content of OPEFB results in fouling, sintering, and agglomeration during high-temperature thermal conversion [40, 41, 66].

Mohammed et al. [66] observed that the particle size of OPEFB in the range 300–1000  $\mu\text{m}$  improved the TPCs and thermal decomposition behaviour of the fuel during conversion. Erlich [257], Erlich, Fransson [258] also examined the effect of the shape, size, and density of OPEFB on the chemical composition and reactivity during thermal conversion. The results demonstrated that low moisture content, size reduction, and pelletisation improved the composition, distribution, and calorific heating value of the OPEFB biochar and syngas products. The results also demonstrate that comprehensive fuel characterisation and pre-treatment (e.g. pelletisation) improve the overall energy potential of the OPEFB.

Several authors have examined the effect of pelletisation on the fuel and energy potential of OPEFB [241, 250, 259–262]. The characterisation techniques cannot specifically address the factors that hinder biomass conversion into bio-based products. However, the knowledge of the chemical, thermal, kinetic, and thermodynamic fuel properties of OPEFB can enhance its energy potential. The fuel characteristics, energy potential, and convertibility of potential of OPEFB can be improved through pre-treatment [263]. Pre-treatment techniques such as drying, size reduction, and pelletisation are energy-intensive, time-consuming, and expensive processes. These drawbacks increase the cost of pre-treatment, conversion, and overall competitiveness of biomass. However, the use of modern drying techniques such as hot flue gases or waste heat presents health, safety, and

environmental risks. The hot flue gas approach also contributes to increased volatile organic compound (VOC) emissions [208], browning, dust explosions, and other safety concerns [264]. Evidence of such risks is ascribed to chemical erosion, fires, explosions, and non-uniform moisture as extensively documented by various researchers [210, 265–268]. The use of pulverised biomass with heterogeneous distribution also causes hot spots, bridging, and clogging in gasifiers during thermal conversion [256, 269].

The pelletisation process is also prone to various challenges. Despite its advantages, the pelletised fuels are prone to grindability and hygroscopicity issues along with breakage as reported in the literature [230, 270]. The thermal conversion of pelletised fuels is prone to delayed ignition, poor gasifier efficiency, smouldering, and low heating value syngas product during gasification [258, 271], which is attributed to heat and mass transport limitations [272]. The poor conversion efficiencies of pellets in biomass reactors result in the emission of particulate matter (PM), pollutant gases, and unoxidised compounds [273, 274]. Other studies have revealed that the long-term storage of pelletised fuels results in the emission of volatile organic compounds (VOCs) through the phenomena known as off-gassing [275, 276]. The process typically results in the depletion of oxygen and emission of hazardous gases such as carbon monoxide (CO) beyond the permitted 35-ppm safety limits [274, 277, 278]. Other studies have confirmed that the long-term storage of biomass pellets irrespective of product quality can affect indoor air quality and pose significant risks to human health, safety and the environment. Despite improvements in quality after pre-treatment, biomass feedstocks still require conversion through various biomass conversion technologies.

## 5 Future outlook and applications

The utilisation of biomass for energy and other low carbon applications is set to increase over the years due to rising

global awareness on the challenges posed by fossil fuels to humans and the environment. The transition from fossil to clean energy sources such as biomass will help to address global warming and climate change as highlighted in the Paris Climate Accord. Biomass could help achieve the goals of the agreement through the diversification of the global energy mix. This will be particularly crucial in developing countries such as Malaysia, Indonesia, Colombia, Thailand, and Nigeria, which have abundant biomass in the form of the oil palm mill and plantation wastes. As highlighted in the National Biomass Strategy (NBS-2020) and the 5<sup>th</sup> Fuel Policy (5FP) of the 8<sup>th</sup> Malaysia Plan (8MP), the valorisation of OPW is crucial to the establishment of a low carbon economy, energy mix diversification, and energy self-sufficiency. However, the poor fuel properties and technical challenges encountered with OPW pre-treatment need to be addressed to ensure an effective transition from the fossil fuel economy. To achieve this, the scientific community and other stakeholders will need to design, develop, and adopt effective strategies for the characterisation, pre-treatment, and valorisation.

Current studies on the characterisation of oil palm wastes aim to examine and highlight the chemical, thermal, kinetic, and thermodynamic properties with limited consideration of the physical properties. The physical characterisation of biomass feedstock provides insights on the properties such as bulk densities, porosity (sphericity), grindability, and particle size distribution. The enumerated parameters are crucial to estimating the biomass characteristics, energy density, and fuel value indices [279, 280]. Studies on the physical properties could also provide forehand information on the suitability of the OPW for selected biomass application and design of conversion equipment along with protocols for safety during handling, storage, or transportation. Future studies need to include characterisation of the physical fuel properties of potential biomass feedstock. Studies on the morphological and microstructural properties using microscopic techniques such as scanning electron microscopy (SEM), transmission electron microscopy (TEM), and energy-dispersive X-ray (EDX) spectroscopy could also present valuable insights into the physical and chemical (or combined physicochemical) fuel properties of OPEFB.

## 6 Conclusions

The paper presented a concise review of the fuel characterisation techniques and pre-treatment technologies for oil palm empty fruit bunches (OPEFB). The current challenges and prospects of pre-treating and characterising OPEFB are also presented in detail in the paper. The findings reveal that the studies on OPEFB characterisation in the literature are typically limited to the chemical, thermal, kinetic, and thermodynamic fuel properties. The authors recommend that future

studies should also critically examine the physical, morphological, and microstructural properties of OPEFB based on gravimetric, spectroscopic, and microscopic techniques such as bulk density, SEM, TEM, and EDX such as bulk density, porosity, energy density, and microstructure among others. The paper also highlights the need for pre-treatment to ensure efficient valorisation of OPEFB and address the challenges associated with its poor fuel properties. The most common pre-treatment techniques for OPEFB in the literature are drying, size reduction (comprising pulverisation, grinding, chipping, and chunking), and pelletisation.

**Acknowledgements** The authors gratefully acknowledge the Centre of Hydrogen Energy, Institute of Future Energy, and the University-Industry Research Laboratory (UIRL) all at the Universiti Teknologi Malaysia (UTM) Skudai Campus in Johor.

## References

- Mutsaers H (2019) The challenge of the oil palm: using degraded land for its cultivation. *Outlook Agric* 48(3):190–197
- Forster BP, Sitepu B, Setiawati U, Kelanaputra ES, Nur F, Rusfiandi H, Rahmah S, Ciomas J, Anwar Y, Bahri S (2017) Oil palm (*Elaeis guineensis*). In: Genetic improvement of tropical crops. Springer, Cham, pp 241–290. [https://doi.org/10.1007/978-3-319-59819-2\\_8](https://doi.org/10.1007/978-3-319-59819-2_8)
- Mohammed M, Salmiaton A, Azlina WW, Amran MM, Fakhru'l-Razi A, Taufiq-Yap Y (2011) Hydrogen rich gas from oil palm biomass as a potential source of renewable energy in Malaysia. *Renew Sust Energ Rev* 15(2):1258–1270
- MPOB (2016) Malaysian Oil Palm Statistics. Malaysian Palm Oil Board (MPOB), Selangor
- Yan W (2017) A makeover for the world's most hated crop. *Nature* 543(1):306–308. <https://doi.org/10.1038/543306a>
- Corley RHV, Tinker PB (2008) The oil palm. World Agriculture Series, 4th edn. Wiley, Bath
- Mekhilef S, Saidur R, Safari A, Mustaffa W (2011) Biomass energy in Malaysia: current state and prospects. *Renew Sust Energ Rev* 15(7):3360–3370
- AIM (2011) National Biomass Strategy 2020: New wealth creation for Malaysia's Palm Oil industry. Agensi Inovasi Malaysia, Putrajaya
- Basiron Y (2007) Palm oil production through sustainable plantations. *Eur J Lipid Sci Technol* 109(4):289–295
- Johari A, Nyakuma BB, Nor SHM, Mat R, Hashim H, Ahmad A, Zakaria ZY, Abdullah TAT (2015) The challenges and prospects of palm oil-based biodiesel in Malaysia. *Energy* 81:255–261
- Mahlia TMI, Ismail N, Hossain N, Silitonga AS, Shamsuddin AH (2019) Palm oil and its wastes as bioenergy sources: a comprehensive review. *Environ Sci Pollut Res* 26:14849–14866. <https://doi.org/10.1007/s11356-019-04563-x>
- MPOB (2019) Overview of the Malaysian Oil Palm Industry 2018. Palm Oil Statistics. Malaysian Palm Oil Board (MPOB), Kuala Lumpur
- National Biomass Strategy (2013) New wealth creation for Malaysia's biomass industry. NBS-2020, vol 2, 2nd edn. Agensi Inovasi Malaysia (AIM), Kuala Lumpur
- Abdullah N, Sulaiman F (2013) The oil palm wastes in Malaysia. In: Biomass now-sustainable growth and use, vol 1. InTech Open Publishers, Rijeka, pp 75–93

15. Hassan MA, Ahmad Farid MA, Shirai Y, Ariffin H, Othman MR, Samsudin MH, Hasan MY (2019) Oil palm biomass biorefinery for sustainable production of renewable materials. *Biotechnol J* 14(6):1800394
16. Bazmi AA, Zahedi G, Hashim H (2011) Progress and challenges in utilization of palm oil biomass as fuel for decentralized electricity generation. *Renew Sust Energy Rev* 15(1):574–583
17. Samiran NA, Jaafar MNM, Ng J-H, Lam SS, Chong CT (2016) Progress in biomass gasification technique—with a focus on Malaysian palm biomass for syngas production. *Renew Sust Energy Rev* 62:1047–1062
18. Loh SK (2017) The potential of the Malaysian oil palm biomass as a renewable energy source. *Energy Convers Manag* 141:285–298
19. Chang SH (2014) An overview of empty fruit bunch from oil palm as feedstock for bio-oil production. *Biomass Bioenergy* 62:174–181. <https://doi.org/10.1016/j.biombioe.2014.01.002>
20. Mohammad N, Alam MZ, Kabbashi NA, Ahsan A (2012) Effective composting of oil palm industrial waste by filamentous fungi: a review. *Resour Conserv Recycl* 58:69–78. <https://doi.org/10.1016/j.resconrec.2011.10.009>
21. Anyaoha KE, Sakrabani R, Patchigolla K, Mouazen AM (2018) Critical evaluation of oil palm fresh fruit bunch solid wastes as soil amendments: prospects and challenges. *Resour Conserv Recycl* 136:399–409. <https://doi.org/10.1016/j.resconrec.2018.04.022>
22. Sohni S, Norulami NAN, Hashim R, Khan SB, Fadhullah W, Omar AKM (2018) Physicochemical characterization of Malaysian crop and agro-industrial biomass residues as renewable energy resources. *Ind Crop Prod* 111:642–650. <https://doi.org/10.1016/j.indcrop.2017.11.031>
23. Uemura Y, Sellappah V, Trinh TH, Hassan S, K-i T (2017) Torrefaction of empty fruit bunches under biomass combustion gas atmosphere. *Bioresour Technol* 243:107–117
24. Sukiran MA, Daud WMAW, Abnisa F, Nasrin AB, Astimar AA, Loh SK (2020) Individual torrefaction parameter enhances characteristics of torrefied empty fruit bunches. *Biomass Convers Biorefinery*. <https://doi.org/10.1007/s13399-020-00804-z>
25. Lee XJ, Lee LY, Gan S, Thangalazhy-Gopakumar S, Ng HK (2017) Biochar potential evaluation of palm oil wastes through slow pyrolysis: thermochemical characterization and pyrolytic kinetic studies. *Bioresour Technol* 236:155–163. <https://doi.org/10.1016/j.biortech.2017.03.105>
26. Francis Prashanth P, Midhun Kumar M, Vinu R (2020) Analytical and microwave pyrolysis of empty oil palm fruit bunch: kinetics and product characterization. *Bioresour Technol* 310:123394. <https://doi.org/10.1016/j.biortech.2020.123394>
27. Zaini IN, Novianti S, Nurdiawati A, Irhamna AR, Aziz M, Yoshikawa K (2017) Investigation of the physical characteristics of washed hydrochar pellets made from empty fruit bunch. *Fuel Process Technol* 160:109–120. <https://doi.org/10.1016/j.fuproc.2017.02.020>
28. Yeoh K-H, Shafie S, Al-Attab K, Zainal Z (2018) Upgrading agricultural wastes using three different carbonization methods: thermal, hydrothermal and vapothermal. *Bioresour Technol* 265:365–371
29. Lee JH, Lee JH, Kim DK, Park CH, Yu JH, Lee EY (2016) Crude glycerol-mediated liquefaction of empty fruit bunches saccharification residues for preparation of biopolyurethane. *J Ind Eng Chem* 34:157–164. <https://doi.org/10.1016/j.jiec.2015.11.007>
30. Miyata Y, Sagata K, Hirose M, Yamazaki Y, Nishimura A, Okuda N, Arita Y, Hirano Y, Kita Y (2017) Fe-assisted hydrothermal liquefaction of lignocellulosic biomass for producing high-grade bio-oil. *ACS Sustain Chem Eng* 5(4):3562–3569. <https://doi.org/10.1021/acssuschemeng.7b00381>
31. Ariffin MA, Mahmood WMFW, Harun Z, Mohamed R (2017) Medium-scale gasification of oil palm empty fruit bunch for power generation. *J Mater Cycles Waste Manag* 19(3):1244–1252. <https://doi.org/10.1007/s10163-016-0518-8>
32. Al-Obaidi M, Ishak NS, Ali S, Karim A, Yun Hin TY (2020) The evaluation on three types of Malaysian dolomites as a primary catalyst in gasification reaction of EFB and tar cracking efficiency. *Front Energy Res* 8:38
33. Uddin Monir M, Abd Aziz A, Vo D-VN, Khatun F (2020) Enhanced hydrogen generation from empty fruit bunches by charcoal addition into a downdraft gasifier. *Chem Eng Technol* 43(4):762–769
34. Madhiyanon T, Sathitruangsak P, Sungworagarn S, Pipatmanomai S, Tia S (2012) A pilot-scale investigation of ash and deposition formation during oil-palm empty-fruit-bunch (EFB) combustion. *Fuel Process Technol* 96:250–264. <https://doi.org/10.1016/j.fuproc.2011.12.020>
35. Parshetti GK, Hoekman SK, Balasubramanian R (2013) Chemical, structural and combustion characteristics of carbonaceous products obtained by hydrothermal carbonization of palm empty fruit bunches. *Bioresour Technol* 135:683–689
36. Ninduangdee P, Kuprianov VI (2016) A study on combustion of oil palm empty fruit bunch in a fluidized bed using alternative bed materials: performance, emissions, and time-domain changes in the bed condition. *Appl Energy* 176(1):34–48
37. Sompong O, Boe K, Angelidaki I (2012) Thermophilic anaerobic co-digestion of oil palm empty fruit bunches with palm oil mill effluent for efficient biogas production. *Appl Energy* 93:648–654
38. Suksong W, Jehlee A, Singkhala A, Kongjan P, Prasertsan P, Imai T, Sompong O (2017) Thermophilic solid-state anaerobic digestion of solid waste residues from palm oil mill industry for biogas production. *Ind Crop Prod* 95:502–511
39. Suksong W, Mamimin C, Prasertsan P, Kongjan P, Sompong O (2019) Effect of inoculum types and microbial community on thermophilic and mesophilic solid-state anaerobic digestion of empty fruit bunches for biogas production. *Ind Crop Prod* 133:193–202
40. Lahijani P, Zainal Z (2014) Fluidized bed gasification of palm empty fruit bunch using various bed materials. *Energy Sources A Recover Utilization Environ Effects* 36(22):2502–2510
41. Lahijani P, Zainal ZA (2011) Gasification of palm empty fruit bunch in a bubbling fluidized bed: a performance and agglomeration study. *Bioresour Technol* 102(2):2068–2076. <https://doi.org/10.1016/j.biortech.2010.09.101>
42. Nyakuma BB, Wong S, Oladokun O (2019) Non-oxidative thermal decomposition of oil palm empty fruit bunch pellets: fuel characterisation, thermogravimetric, kinetic, and thermodynamic analyses. *Biomass Convers Biorefinery*. <https://doi.org/10.1007/s13399-13019-00568-13391>
43. Mohammed MAA, Salmiaton A, Azlina WAKGW, Amran MSM, Fakhru'l-Razi A, Taufiq-Yap YH (2011) Hydrogen rich gas from oil palm biomass as a potential source of renewable energy in Malaysia. *Renew Sustain Energy Rev* 15(2):1258–1270. <https://doi.org/10.1016/j.rser.2010.10.003>
44. Hosseini SE, Wahid MA (2014) Utilization of palm solid residue as a source of renewable and sustainable energy in Malaysia. *Renew Sustain Energy Rev* 40:621–632. <https://doi.org/10.1016/j.rser.2014.07.214>
45. Samiran NA, Jaafar MNM, Chong CT, Jo-Han N (2015) A review of palm oil biomass as a feedstock for syngas fuel technology. *J Teknol* 72(5):13–18
46. Pogaku R, Hardinge BS, Vuthaluru H, Amir HA (2016) Production of bio-oil from oil palm empty fruit bunch by catalytic fast pyrolysis: a review. *Biofuels-Uk* 7(6):647–660. <https://doi.org/10.1080/17597269.2016.1187539>
47. Hamzah N, Tokimatsu K, Yoshikawa K (2019) Solid fuel from oil palm biomass residues and municipal solid waste by hydrothermal

- treatment for electrical power generation in Malaysia: a review. Sustainability 11(4). <https://doi.org/10.3390/su11041060>
48. Akhtar J, Teo CL, Lai LW, Hassan N, Idris A, Abd Aziz R (2015) Factors affecting delignification of oil palm empty fruit bunch by microwave-assisted dilute acid/alkali pretreatment. *Bioresources* 10(1):588–596
  49. Isoni V, Kumbang A, Sharratt PN, Khoo HH (2018) Biomass to levulinic acid: a techno-economic analysis and sustainability of biorefinery processes in Southeast Asia. *J Environ Manag* 214: 267–275. <https://doi.org/10.1016/j.jenvman.2018.03.012>
  50. Ahmad FB, Zhang Z, Doherty WOS, O'Hara IM (2019) The outlook of the production of advanced fuels and chemicals from integrated oil palm biomass biorefinery. *Renew Sustain Energy Rev* 109:386–411. <https://doi.org/10.1016/j.rser.2019.04.009>
  51. Ferrer A, Vega A, Ligeró P, Rodríguez A (2011) Pulping of empty fruit bunches (EFB) from the palm oil industry by formic acid. *Bioresources* 6(4):4282–4301
  52. Khalil HPSA, Marliana MM, Alshammari T (2011) Material properties of epoxy-reinforced biocomposites with lignin from empty fruit bunch as curing agent. *Bioresources* 6(4):5206–5223
  53. Padzil FNM, Lee SH, Ainun ZMA, Lee CH, Abdullah LC (2020) Potential of oil palm empty fruit bunch resources in nanocellulose hydrogel production for versatile applications: a review. *Materials* 13(5):26. <https://doi.org/10.3390/ma13051245>
  54. Narapakdeesakul D, Sridach W, Wittaya T (2013) Novel use of oil palm empty fruit bunch's lignin derivatives for the production of linerboard coating. *Prog Org Coat* 76(7-8):999–1005. <https://doi.org/10.1016/j.porgcoat.2013.02.015>
  55. Bhat IUH, Khalil H, Ismail H, Alshammari T (2011) Morphological, spectroscopic, and thermal properties of alkali-treated and chemically modified oil palm empty fruit bunch fibres and oil palm frond fibres: a comparative study. *Bioresources* 6(4): 4673–4685
  56. Hassan A, Salema AA, Ani FN, Abu Baker A (2010) A review on oil palm empty fruit bunch fiber-reinforced polymer composite materials. *Polym Compos* 31(12):2079–2101. <https://doi.org/10.1002/pc.21006>
  57. Mahjoub R, Yatim JB (2013) Sam ARM (2013) A review of structural performance of oil palm empty fruit bunch fiber in polymer composites. *Adv Mater Sci Eng.* <https://doi.org/10.1155/2013/415359>
  58. Sims REH (2002) The brilliance of bioenergy: in Business and practice. Earthscan Publications Ltd, London
  59. Cai J, He Y, Yu X, Banks SW, Yang Y, Zhang X, Yu Y, Liu R, Bridgwater AV (2017) Review of physicochemical properties and analytical characterization of lignocellulosic biomass. *Renew Sust Energy Rev* 76:309–322
  60. Oladokun O, Ahmad A, Abdullah T, Nyakuma B, Bello A-H, Al-Shatri A (2016) Multicomponent devolatilization kinetics and thermal conversion of *imperata cylindrica*. *Appl Therm Eng* 105:931–940
  61. Basu P (2010) Biomass gasification and pyrolysis: practical design and theory. Academic Press (Elsevier), Burlington
  62. Crocker M (2010) Thermochemical conversion of biomass to liquid fuels and chemicals. RSC Energy and Environment series, vol 1. Royal Society of Chemistry (RSC), London
  63. Yang H, Yan R, Chen H, Lee DH, Liang DT, Zheng C (2006) Pyrolysis of palm oil wastes for enhanced production of hydrogen-rich gases. *Fuel Process Technol* 87(10):935–942. <https://doi.org/10.1016/j.fuproc.2006.07.001>
  64. Abdullah N, Gerhauser H (2008) Bio-oil derived from empty fruit bunches. *Fuel* 87(12):2606–2613
  65. Li J, Yin Y, Zhang X, Liu J, Yan R (2009) Hydrogen-rich gas production by steam gasification of palm oil wastes over supported tri-metallic catalyst. *Int J Hydrog Energy* 34(22):9108–9115
  66. Mohammed MAA, Salmiaton A, Wan Azlina WAKG, Mohamad Amran MS (2012) Gasification of oil palm empty fruit bunches: a characterization and kinetic study. *Bioresour Technol* 110(0):628–636. <https://doi.org/10.1016/j.biortech.2012.01.056>
  67. Langè S, Pellegrini LA (2013) Economic analysis of combined production of hydrogen-energy from empty fruit bunches. *Biomass Bioenergy* 59:520–531. <https://doi.org/10.1016/j.biombioe.2013.08.039>
  68. Parshetti GK, Quek A, Betha R, Balasubramanian R (2014) TGA–FTIR investigation of co-combustion characteristics of blends of hydrothermally carbonized oil palm biomass (EFB) and coal. *Fuel Process Technol* 118:228–234. <https://doi.org/10.1016/j.fuproc.2013.09.010>
  69. Johari A, Abdullah T, Amran T, Hassim MH, Kidam K, Kamaruddin MJ, Zakaria ZY, Sulaiman WRW (2015) Effect of fluidization number on the combustion of empty fruit bunch in a fluidized bed. In: *Adv Mater Res. Trans Tech Publ*, pp 301–305
  70. Chan YH, Yusup S, Quitain AT, Tan RR, Sasaki M, Lam HL, Uemura Y (2015) Effect of process parameters on hydrothermal liquefaction of oil palm biomass for bio-oil production and its life cycle assessment. *Energy Convers Manag* 104:180–188
  71. Aziz M, Prawisudha P, Prabowo B, Budiman BA (2015) Integration of energy-efficient empty fruit bunch drying with gasification/combined cycle systems. *Appl Energy* 139:188–195
  72. Chuah LF, Amin MM, Yusup S, Bokhari A, Klemeš JJ, Alnarabiji MS (2016) Influence of green catalyst on transesterification process using ultrasonic-assisted. *J Clean Prod* 136:14–22
  73. Nakason K, Panyapinyopol B, Kanokkantapong V, Viriyapempikul N, Kraithong W, Pavasant P (2017) Hydrothermal carbonization of oil palm pressed fiber: effect of reaction parameters on product characteristics. *Int Energy J* 17(2):47–56
  74. Hantoko D, Yan M, Prabowo B, Susanto H (2018) Preparation of empty fruit bunch as a feedstock for gasification process by employing hydrothermal treatment. *Energy Procedia* 152:1003–1008
  75. Yan M, Hantoko D, Susanto H, Ardy A, Waluyo J, Weng Z, Lin J (2019) Hydrothermal treatment of empty fruit bunch and its pyrolysis characteristics. *Biomass Convers Biorefinery* 9(4):709–717
  76. Johari A, Hashim H, Ramli M, Jusoh M, Rozainee M (2011) Effects of fluidization number and air factor on the combustion of mixed solid waste in a fluidized bed. *Appl Therm Eng* 31(11): 1861–1868
  77. Basu P (2006) Combustion and gasification in fluidized beds. CRC Press, Burlington
  78. Channiwala SA, Parikh PP (2002) A unified correlation for estimating HHV of solid, liquid and gaseous fuels. *Fuel* 81(8):1051–1063. [https://doi.org/10.1016/S0016-2361\(01\)00131-4](https://doi.org/10.1016/S0016-2361(01)00131-4)
  79. Friedl A, Padouvas E, Rotter H, Varmuza K (2005) Prediction of heating values of biomass fuel from the elemental composition. *Anal Chim Acta* 544(1):191–198
  80. Baskar C, Baskar S, Dhillon RS (2012) Biomass conversion: the interface of biotechnology, chemistry and materials science. Springer Science & Business Media.
  81. Donahue CJ, Rais EA (2009) Proximate analysis of coal. *J Chem Educ* 86(2):222. <https://doi.org/10.1021/ed086p222>
  82. Basu P (2018) Biomass gasification, pyrolysis and torrefaction: practical design and theory, vol 2. Academic Press (Elsevier), London
  83. Ninduangdee P, Kuprianov VI, Cha EY, Kaewrath R, Youngyuen P, Atthawethworawuth W (2015) Thermogravimetric studies of oil palm empty fruit bunch and palm kernel shell: TG/DTG analysis and modelling. *Energy Procedia* 79:453–458
  84. Shahbaz M, Yusup S, Naz M, Sulaiman S, Inayat A, Partama A (2017) Fluidization of palm kernel shell, palm oil fronds, and

- empty fruit bunches in a swirling fluidized bed gasifier. *Part Sci Technol* 35(2):150–157
85. Kieseler S, Neubauer Y, Zobel N (2013) Ultimate and proximate correlations for estimating the higher heating value of hydrothermal solids. *Energy Fuel* 27(2):908–918
  86. Nhuchhen DR, Salam PA (2012) Estimation of the higher heating value of biomass from the proximate analysis: a new approach. *Fuel* 99:55–63
  87. Parikh J, Channiwala S, Ghosal G (2005) A correlation for calculating HHV from proximate analysis of solid fuels. *Fuel* 84(5):487–494
  88. Lakhundi S, Siddiqui R, Khan NA (2015) Cellulose degradation: a therapeutic strategy in the improved treatment of *Acanthamoeba* infections. *Parasit Vectors* 8(1):23. <https://doi.org/10.1186/s13071-015-0642-7>
  89. dos Santos AC, Ximenes E, Kim Y, Ladisch MR (2019) Lignin–enzyme interactions in the hydrolysis of lignocellulosic biomass. *Trends Biotechnol* 37(5):518–531
  90. Pang Z, Lyu W, Dong C, Li H, Yang G (2016) High selective delignification using oxidative ionic liquid pretreatment at mild conditions for efficient enzymatic hydrolysis of lignocellulose. *Bioresour Technol* 214:96–101
  91. Ling Z, Chen S, Zhang X, Xu F (2017) Exploring crystalline-structural variations of cellulose during alkaline pretreatment for enhanced enzymatic hydrolysis. *Bioresour Technol* 224:611–617
  92. Diebold J, Bridgwater AV (1997) Overview of fast pyrolysis of biomass for the production of liquid fuels. In: Bridgwater AV, Boocock DGB (Eds) *Developments in thermochemical biomass conversion*. Springer, Dordrecht, pp 5–23. [https://doi.org/10.1007/978-94-009-1559-6\\_1](https://doi.org/10.1007/978-94-009-1559-6_1)
  93. Sricharoenchaikul V, Atong D (2009) Thermal decomposition study on *Jatropha curcas* L. waste using TGA and fixed bed reactor. *J Anal Appl Pyrolysis* 85(1):155–162. <https://doi.org/10.1016/j.jaap.2008.11.030>
  94. Chio C, Sain M, Qin W (2019) Lignin utilization: a review of lignin depolymerization from various aspects. *Renew Sust Energ Rev* 107:232–249
  95. Ragauskas AJ, Beckham GT, Bidy MJ, Chandra R, Chen F, Davis MF, Davison BH, Dixon RA, Gilna P, Keller M (2014) Lignin valorization: improving lignin processing in the biorefinery. *Science* 344(6185):1246843. <https://doi.org/10.1126/science.1246843>
  96. Vanholme R, Demedts B, Morreel K, Ralph J, Boerjan W (2010) Lignin biosynthesis and structure. *Plant Physiol* 153(3):895–905
  97. Sun R, Tomkinson J, Bolton J (1999) Effects of precipitation pH on the physicochemical properties of the lignins isolated from the black liquor of oil palm empty fruit bunch fibre pulping. *Polym Degrad Stab* 63(2):195–200. [https://doi.org/10.1016/S0141-3910\(98\)00091-3](https://doi.org/10.1016/S0141-3910(98)00091-3)
  98. Farooq M, Zou T, Riviere G, Sipponen MH, Österberg M (2018) Strong, ductile, and waterproof cellulose nanofibril composite films with colloidal lignin particles. *Biomacromolecules* 20(2):693–704
  99. Smith MD, Mostofian B, Cheng X, Petridis L, Cai CM, Wyman CE, Smith JC (2016) Cosolvent pretreatment in cellulosic biofuel production: effect of tetrahydrofuran–water on lignin structure and dynamics. *Green Chem* 18(5):1268–1277
  100. Siqueira G, Arantes V, Saddler JN, Ferraz A, Milagres AM (2017) Limitation of cellulose accessibility and unproductive binding of cellulases by pretreated sugarcane bagasse lignin. *Biotechnol Biofuels* 10(1):1–12
  101. Kelly-Yong TL, Lee KT, Mohamed AR, Bhatia S (2007) Potential of hydrogen from oil palm biomass as a source of renewable energy worldwide. *Energy Policy* 35(11):5692–5701
  102. Palamae S, Dechatiwongse P, Choerit W, Chisti Y, Prasertsan P (2017) Cellulose and hemicellulose recovery from oil palm empty fruit bunch (EFB) fibres and production of sugars from the fibres. *Carbohydr Polym* 155:491–497. <https://doi.org/10.1016/j.carbpol.2016.09.004>
  103. Rodríguez A, Serrano L, Moral A, Pérez A, Jiménez L (2008) Use of high-boiling point organic solvents for pulping oil palm empty fruit bunches. *Bioresour Technol* 99(6):1743–1749
  104. Ishola MM, Millati R, Syamsiah S, Cahyanto MN, Niklasson C, Taherzadeh MJ (2012) Structural changes of oil palm empty fruit bunch (OPEFB) after fungal and phosphoric acid pretreatment. *Molecules* 17(12):14995–15012
  105. Isroi CA, Panji T, Wibowo NA, Syamsu K (2017) Bioplastic production from the cellulose of oil palm empty fruit bunch. In: *IOP Conference Series: Earth and Environmental Science*, vol 12011, pp 1755–1315
  106. Barlianti V, Dahnum D, Hendarsyah H, Abimanyu H (2015) Effect of alkaline pretreatment on properties of lignocellulosic oil palm waste. *Procedia Chem* 16:195–201. <https://doi.org/10.1016/j.proche.2015.12.036>
  107. Hamzah F, Idris A, Shuan TK (2011) Preliminary study on enzymatic hydrolysis of treated oil palm (*Elaeis*) empty fruit bunches fibre (EFB) by using a combination of cellulase and  $\beta$  1-4 glucosidase. *Biomass Bioenergy* 35(3):1055–1059. <https://doi.org/10.1016/j.biombioe.2010.11.020>
  108. Zakaria MR, Fujimoto S, Hirata S, Hassan MA (2014) Ball milling pretreatment of oil palm biomass for enhancing enzymatic hydrolysis. *Appl Biochem Biotechnol* 173(7):1778–1789
  109. Rashid T, Gnanasundaram N, Appusamy A, Kait CF, Thanabalan M (2018) Enhanced lignin extraction from different species of oil palm biomass: kinetics and optimization of extraction conditions. *Ind Crop Prod* 116:122–136. <https://doi.org/10.1016/j.indcrop.2018.02.056>
  110. Demirbas A (2009) Biofuels securing the planet’s future energy needs. *Energy Convers Manag* 50(9):2239–2249
  111. Zhang L, Xu CC, Champagne P (2010) Overview of recent advances in thermo-chemical conversion of biomass. *Energy Convers Manag* 51(5):969–982
  112. Vamvuka D, Kakaras E (2011) Ash properties and environmental impact of various biomass and coal fuels and their blends. *Fuel Process Technol* 92(3):570–581
  113. Suopajarvi H, Pongrácz E, Fabritius T (2013) The potential of using biomass-based reducing agents in the blast furnace: a review of thermochemical conversion technologies and assessments related to sustainability. *Renew Sust Energ Rev* 25:511–528
  114. Carpenter D, Westover TL, Czernik S, Jablonski W (2014) Biomass feedstocks for renewable fuel production: a review of the impacts of feedstock and pretreatment on the yield and product distribution of fast pyrolysis bio-oils and vapours. *Green Chem* 16(2):384–406
  115. Demirbas A (2005) Potential applications of renewable energy sources, biomass combustion problems in boiler power systems and combustion related environmental issues. *Prog Energy Combust Sci* 31(2):171–192. <https://doi.org/10.1016/j.pecs.2005.02.002>
  116. Nunes L, Matias J, Catalão J (2016) Biomass combustion systems: a review on the physical and chemical properties of the ashes. *Renew Sust Energ Rev* 53:235–242
  117. Vamvuka D, Zografos D, Alevizos G (2008) Control methods for mitigating biomass ash-related problems in fluidized beds. *Bioresour Technol* 99(9):3534–3544
  118. Mettanan V, Basu P, Butler J (2009) Agglomeration of biomass-fired fluidized bed gasifier and combustor. *Can J Chem Eng* 87(5):656–684
  119. Teixeira P, Lopes H, Gulyurtlu I, Lapa N, Abelha P (2012) Evaluation of slagging and fouling tendency during biomass co-firing with coal in a fluidized bed. *Biomass Bioenergy* 39(1):192–203

120. Le DM, Sørensen HR, Meyer AS (2017) Elemental analysis of various biomass solid fractions in biorefineries by X-ray fluorescence spectrometry. *Biomass Bioenergy* 97:70–76
121. Wang Z, Mai K, Kumar N, Elder T, Groom LH, Spivey JJ (2017) Effect of steam during Fischer–Tropsch synthesis using biomass-derived syngas. *Catal Lett* 147(1):62–70
122. Arun S, Manikandan NA, Pakshirajan K, Pugazhenth G, Syiem MB (2017) Cu (II) removal by *Nostoc muscorum* and its effect on biomass growth and nitrate uptake: a photobioreactor study. *Int Biodeterior Biodegradation* 119:111–117
123. Clery DS, Mason PE, Rayner CM, Jones JM (2018) The effects of an additive on the release of potassium in biomass combustion. *Fuel* 214:647–655
124. Asadieraghi M, Daud WMAW (2014) Characterization of lignocellulosic biomass thermal degradation and physicochemical structure: effects of demineralization by diverse acid solutions. *Energy Convers Manag* 82:71–82
125. Fukuda S (2015) Pyrolysis investigation for bio-oil production from various biomass feedstocks in Thailand. *Int J Green Energy* 12(3):215–224
126. Kadir A, Sarani N, Abdullah M, Perju M, Sandu A (2017) Study on fired clay bricks by replacing clay with palm oil waste: effects on physical and mechanical properties. In: IOP Conference Series: Materials Science and Engineering, 1(209):012037. IOP Publishing. <https://doi.org/10.1088/1757-899X/209/1/012037>
127. Viana H, Vega-Nieva D, Torres LO, Lousada J, Aranha J (2012) Fuel characterization and biomass combustion properties of selected native woody shrub species from central Portugal and NW Spain. *Fuel* 102:737–745
128. Werle S (2014) Impact of feedstock properties and operating conditions on sewage sludge gasification in a fixed bed gasifier. *Waste Manag Res* 32(10):954–960
129. Słopiecka K, Bartocci P, Fantozzi F (2012) Thermogravimetric analysis and kinetic study of poplar wood pyrolysis. *Appl Energy* 97:491–497. <https://doi.org/10.1016/j.apenergy.2011.12.056>
130. Damartzis T, Vamvuka D, Sfakiotakis S, Zabaniotou A (2011) Thermal degradation studies and kinetic modelling of cardoon (*Cynara cardunculus*) pyrolysis using thermogravimetric analysis (TGA). *Bioresour Technol* 102(10):6230–6238. <https://doi.org/10.1016/j.biortech.2011.02.060>
131. Li L, Wang G, Wang S, Qin S (2013) Thermogravimetric and kinetic analysis of energy crop Jerusalem artichoke using the distributed activation energy model. *J Therm Anal Calorim* 114(3):1183–1189. <https://doi.org/10.1007/s10973-013-3115-2>
132. Ceylan S, Topçu Y (2014) Pyrolysis kinetics of hazelnut husk using thermogravimetric analysis. *Bioresour Technol* 156:182–188. <https://doi.org/10.1016/j.biortech.2014.01.040>
133. Wang S, Dai G, Yang H, Luo Z (2017) Lignocellulosic biomass pyrolysis mechanism: a state-of-the-art review. *Prog Energy Combust Sci* 62:33–86
134. Gabbott P (2008) Principles and applications of thermal analysis, 1st edn. Blackwell Publishing Limited, Oxford
135. Fateh T, Richard F, Rogaume T, Joseph P (2016) Experimental and modelling studies on the kinetics and mechanisms of thermal degradation of polymethyl methacrylate in nitrogen and air. *J Anal Appl Pyrolysis* 120:423–433
136. Chen W-H, Kuo P-C (2011) Isothermal torrefaction kinetics of hemicellulose, cellulose, lignin and xylan using thermogravimetric analysis. *Energy* 36(11):6451–6460
137. Chen D, Zheng Y, Zhu X (2012) Determination of effective moisture diffusivity and drying kinetics for poplar sawdust by thermogravimetric analysis under isothermal condition. *Bioresour Technol* 107:451–455
138. Morin M, Pécate S, Masi E, Hémati M (2017) Kinetic study and modelling of char combustion in TGA in isothermal conditions. *Fuel* 203:522–536
139. Luangkiattikhun P, Tangsathitkulchai C, Tangsathitkulchai M (2008) Non-isothermal thermogravimetric analysis of oil-palm solid wastes. *Bioresour Technol* 99(5):986–997. <https://doi.org/10.1016/j.biortech.2007.03.001>
140. El-Sayed SA, Mostafa M (2014) Pyrolysis characteristics and kinetic parameters determination of biomass fuel powders by differential thermal gravimetric analysis (TGA/DTG). *Energy Convers Manag* 85:165–172
141. Sørensen OT, Rouquerol J (2003) Sample controlled thermal analysis: origin, goals, multiple forms, applications and future. Springer US
142. Sørensen OT, Rouquerol J (2003) Sample controlled thermal analysis: origin, goals, multiple forms, applications and future. Springer Science & Business Media, USA. <https://doi.org/10.1007/978-1-4757-3735-6>
143. Varol M, Atımtay A, Bay B, Olgun H (2010) Investigation of co-combustion characteristics of low-quality lignite coals and biomass with thermogravimetric analysis. *Thermochim Acta* 510(1):195–201
144. Yang H, Yan R, Chen H, Lee DH, Zheng C (2007) Characteristics of hemicellulose, cellulose and lignin pyrolysis. *Fuel* 86(12–13):1781–1788. <https://doi.org/10.1016/j.fuel.2006.12.013>
145. Açıklıkın K (2011) Thermogravimetric analysis of walnut shell as pyrolysis feedstock. *J Therm Anal Calorim* 105(1):145–150. <https://doi.org/10.1007/s10973-010-1267-x>
146. Kumar A, Wang L, Dzenis YA, Jones DD, Hanna MA (2008) Thermogravimetric characterization of corn stover as gasification and pyrolysis feedstock. *Biomass Bioenergy* 32(5):460–467. <https://doi.org/10.1016/j.biombioe.2007.11.004>
147. Gašparović L, Koreňová Z, Jelemenský L (2010) Kinetic study of wood chips decomposition by TGA. *Chem Pap* 64(2):174–181
148. Lopez-Velazquez MA, Santes V, Balmaseda J, Torres-Garcia E (2013) Pyrolysis of orange waste: a thermo-kinetic study. *J Anal Appl Pyrolysis* 99:170–177. <https://doi.org/10.1016/j.jaap.2012.09.016>
149. Abovade AO, Hugo TJ, Carrier M, Meyer EL, Stahl R, Knoetze JH, Görgens JF (2011) Non-isothermal kinetic analysis of the devolatilization of corn cobs and sugar cane bagasse in an inert atmosphere. *Thermochim Acta* 517(1–2):81–89. <https://doi.org/10.1016/j.tca.2011.01.035>
150. Yan R, Yang H, Chin T, Liang DT, Chen H, Zheng C (2005) Influence of temperature on the distribution of gaseous products from pyrolyzing palm oil wastes. *Combust Flame* 142(1):24–32
151. Idris SS, Rahman NA, Ismail K, Alias AB, Rashid ZA, Aris MJ (2010) Investigation on thermochemical behaviour of low-rank Malaysian coal, oil palm biomass and their blends during pyrolysis via thermogravimetric analysis (TGA). *Bioresour Technol* 101(12):4584–4592. <https://doi.org/10.1016/j.biortech.2010.01.059>
152. Omar R, Idris A, Yunus R, Khalid K, Isma MA (2011) Characterization of empty fruit bunch for microwave-assisted pyrolysis. *Fuel* 90(4):1536–1544
153. Idris SS, Rahman NA, Ismail K (2012) Combustion characteristics of Malaysian oil palm biomass, sub-bituminous coal and their respective blends via thermogravimetric analysis (TGA). *Bioresour Technol* 123:581–591. <https://doi.org/10.1016/j.biortech.2012.07.065>
154. Izani MN, Paridah M, Anwar U, Nor MM, H'ng P (2013) Effects of fibre treatment on morphology, tensile and thermogravimetric analysis of oil palm empty fruit bunches fibres. *Compos Part B* 45(1):1251–1257
155. Sabil KM, Aziz MA, Lal B, Uemura Y (2013) Effects of torrefaction on the physicochemical properties of oil palm empty

- fruit bunches, mesocarp fiber and kernel shell. *Biomass Bioenergy* 56:351–360
156. Chowdhury M, Mina M, Beg M, Khan MR (2013) Cu nanoparticles for improving the mechanical performances of oil palm empty fruit bunch fibres as analyzed by the Weibull model. *Polym Bull* 70(11):3103–3113
  157. Alias NB, Ibrahim N, Hamid MKA (2014) Pyrolysis of empty fruit bunch by thermogravimetric analysis. *Energy Procedia* 61: 2532–2536
  158. Auta M, Ern L, Hameed B (2014) Fixed-bed catalytic and non-catalytic empty fruit bunch biomass pyrolysis. *J Anal Appl Pyrolysis* 107:67–72
  159. Harmaen AS, Khalina A, Azowa I, Hassan MA, Tarmian A, Jawaid M (2015) Thermal and biodegradation properties of poly (lactic acid)/fertilizer/oil palm fibres blends biocomposites. *Polym Compos* 36(3):576–583
  160. Mohamed AR, Hamzah Z (2015) An alternative approach for the screening of catalytic empty fruit bunch (EFB) pyrolysis using the values of activation energy from a thermogravimetric study. *React Kinet Mech Catal* 114(2):529–545
  161. Dewayanto N, Azman AN, Ahmad NA, Shah MSHM (2016) Study of thermal degradation of biomass wastes generated from palm oil milling plant. *CHEMICA J Teknik Kimia* 3(2):31–37
  162. Novianti S, Nurdawati A, Zaini IN, Sumida H, Yoshikawa K (2016) Hydrothermal treatment of palm oil empty fruit bunches: an investigation of the solid fuel and liquid organic fertilizer applications. *Biofuels* 7(6):627–636
  163. Yahaya ANA, Hossain MS, Edyvean R (2017) Thermal degradation and morphological changes of oil palm empty fruit bunch vermicompost. *BioResources* 12(4):8886–8900
  164. Poudel J, Ohm T-I, Gu JH, Shin MC, Oh SC (2017) Comparative study of torrefaction of empty fruit bunches and palm kernel shell. *J Mater Cycles Waste Manag* 19(2):917–927
  165. Chew J-J, Doshi V, Yong S-T, Bhattacharya S (2016) Kinetic study of torrefaction of oil palm shell, mesocarp and empty fruit bunch. *J Therm Anal Calorim* 126(2):709–715
  166. Maia AAD, de Moraes LC (2016) Kinetic parameters of red pepper waste as biomass to solid biofuel. *Bioresour Technol* 204:157–163
  167. Cai J, Xu D, Dong Z, Yu X, Yang Y, Banks SW, Bridgwater AV (2017) Processing thermogravimetric analysis data for isoconversional kinetic analysis of lignocellulosic biomass pyrolysis: case study of corn stalk. *Renew Sust Energ Rev* 82(3):2705–2715
  168. Jain A, Mehra A, Ranade V (2016) Processing of TGA data: analysis of isoconversional and model fitting methods. *Fuel* 165(1):490–498
  169. Polat S, Apaydin-Varol E, Putun AE (2013) TGA-FTIR study on the thermal decomposition of tea waste. *J Selcuk Univ Nat Appl Sci* 2(2):420–430
  170. Van de Velden M, Baeyens J, Brems A, Janssens B, Dewil R (2010) Fundamentals, kinetics and endothermicity of the biomass pyrolysis reaction. *Renew Energy* 35(1):232–242
  171. Khawam A, Flanagan DR (2005) Complementary use of model-free and modelistic methods in the analysis of solid-state kinetics. *J Phys Chem B* 109(20):10073–10080
  172. Sánchez-Jiménez P, Pérez-Maqueda L, Perejón A, Criado J (2013) Limitations of model-fitting methods for kinetic analysis: polystyrene thermal degradation. *Resour Conserv Recycl* 74(1):75–81
  173. Khawam A (2007) Application of solid-state kinetics to desolvation reactions. University of Iowa, Iowa
  174. Tonbul Y (2007) Pyrolysis of pistachio shell as biomass. *J Therm Anal Calorim* 91(2):641–647
  175. Lu C, Song W, Lin W (2009) Kinetics of biomass catalytic pyrolysis. *Biotechnol Adv* 27(5):583–587
  176. Yorulmaz SY, Atimtay AT (2009) Investigation of combustion kinetics of treated and untreated waste wood samples with thermogravimetric analysis. *Fuel Process Technol* 90(7):939–946
  177. Masnadi MS, Habibi R, Kopyscinski J, Hill JM, Bi X, Lim CJ, Ellis N, Grace JR (2014) Fuel characterization and co-pyrolysis kinetics of biomass and fossil fuels. *Fuel* 117:1204–1214
  178. Poletto M, Zattera AJ, Santana RMC (2012) Thermal decomposition of wood: kinetics and degradation mechanisms. *Bioresour Technol* 126(0):7–12. <https://doi.org/10.1016/j.biortech.2012.08.133>
  179. Cheng G, Zheng Y, Hu ZQ, Xiao B, Cai HY, He PW, Wang JB (2015) Kinetic study on pyrolysis of blooming-forming cyanobacteria. *Energy Sources A Recover Utilization Environ Effects* 37(6):625–632. <https://doi.org/10.1080/15567036.2011.590866>
  180. Mishra RK, Mohanty K (2017) Pyrolysis kinetics and thermal behaviour of waste sawdust biomass using thermogravimetric analysis. *Bioresour Technol* 251(1):63–74
  181. Flynn JH, Wall LA (1966) A quick, direct method for the determination of activation energy from thermogravimetric data. *J Polymer Sci B Polymer Lett* 4(5):323–328. <https://doi.org/10.1002/pol.1966.110040504>
  182. Ozawa T (1965) A new method of analyzing thermogravimetric data. *Bull Chem Soc Jpn* 38(11):1881–1886. <https://doi.org/10.1246/bcsj.38.1881>
  183. Akahira T, Sunose T (1971) Method of determining activation deterioration constant of electrical insulating materials. *Res Rep Chiba Inst Technol (Sci Technol)* 16:22–31
  184. Friedman HL (1964) Kinetics of thermal degradation of char-forming plastics from thermogravimetry. Application to a phenolic plastic. In: *Journal of Polymer Science: Polymer Symposia*. vol 1. Wiley Online Library, pp 183–195
  185. Starink M, Wang P, Sinclair I, Gregson P (1999) Microstructure and strengthening of Al-Li-Cu-Mg alloys and MMCs: II. Modelling of yield strength. *Acta Mater* 47(14):3855–3868
  186. Vyazovkin S (2001) Modification of the integral isoconversional method to account for variation in the activation energy. *J Comput Chem* 22(2):178–183
  187. Cai J, Chen S (2009) A new iterative linear integral isoconversional method for the determination of the activation energy varying with the conversion degree. *J Comput Chem* 30(13):1986–1991
  188. Várhegyi G, Bobály B, Jakab E, Chen H (2010) Thermogravimetric study of biomass pyrolysis kinetics. A distributed activation energy model with prediction tests. *Energy Fuel* 25(1):24–32
  189. Hu RZ, Gao SL (2010) Thermal analysis kinetics
  190. Song C, Ai N, Shan S, Ji J (2013) Catalytic effect of CuCl on pyrolysis of five kinds of biomass. *Energy Sources A Recover Utilization Environ Effects* 35(11):1056–1063. <https://doi.org/10.1080/15567036.2011.650278>
  191. Kissinger HE (1956) Variation of peak temperature with the heating rate in differential thermal analysis. *J Res Natl Bur Stand* 57(4):217–221
  192. Babu B, Chaurasia A (2004) Parametric study of thermal and thermodynamic properties on pyrolysis of biomass in the thermally thick regime. *Energy Convers Manag* 45(1):53–72
  193. Drescher U, Brüggemann D (2007) Fluid selection for the Organic Rankine Cycle (ORC) in biomass power and heat plants. *Appl Therm Eng* 27(1):223–228
  194. Li C, Suzuki K (2009) Tar property, analysis, reforming mechanism and model for biomass gasification—an overview. *Renew Sust Energ Rev* 13(3):594–604
  195. Vasiliu M, Guynn K, Dixon DA (2011) Prediction of the thermodynamic properties of key products and intermediates from biomass. *J Phys Chem C* 115(31):15686–15702







272. Kallis KX, Susini GAP, Oakey JE (2013) A comparison between *Miscanthus* and bioethanol waste pellets and their performance in a downdraft gasifier. *Appl Energy* 101(1):333–340
273. Zhang J, Smith K, Ma Y, Ye S, Jiang F, Qi W, Liu P, Khalil M, Rasmussen R, Thorneloe S (2000) Greenhouse gases and other airborne pollutants from household stoves in China: a database for emission factors. *Atmos Environ* 34(26):4537–4549
274. Johansson LS, Leckner B, Gustavsson L, Cooper D, Tullin C, Potter A (2004) Emission characteristics of modern and old-type residential boilers fired with wood logs and wood pellets. *Atmos Environ* 38(25):4183–4195
275. Arshadi M, Gref R (2005) Emission of volatile organic compounds from softwood pellets during storage. *For Prod J* 55(12):132–135
276. Kuang X, Shankar TJ, Bi XT, Sokhansanj S, Lim CJ, Melin S (2008) Characterization and kinetics study of off-gas emissions from stored wood pellets. *Ann Occup Hyg* 52(8):675–683. <https://doi.org/10.1093/annhyg/men053>
277. Svedberg U, Samuelsson J, Melin S (2008) Hazardous off-gassing of carbon monoxide and oxygen depletion during ocean transportation of wood pellets. *Ann Occup Hyg* 52(4):259–266. <https://doi.org/10.1093/annhyg/men013>
278. Soto-Garcia L, Huang X, Thimmaiah D, Rossner A, Hopke PK (2014) Exposures to carbon monoxide from off-gassing of bulk stored wood pellets. *Energy Fuel* 29(1):218–226
279. Hossain N (2020) Characterization of novel moss biomass, *Bryum dichotomum* Hedw. as solid fuel feedstock. *BioEnergy Res* 13(1):50–60. <https://doi.org/10.1007/s12155-019-10086-7>
280. Boundy RG, Davis SC (2010) Biomass energy data book: Edition 4. Oak Ridge National Laboratory (ORNL), Oak Ridge

**Publisher's Note** Springer Nature remains neutral with regard to jurisdictional claims in published maps and institutional affiliations.